

**ULTRASTRUCTURAL MALFORMATIONS OF THE CEREBRAL
MICROVESSELS IN PATHOLOGICAL CONDITIONS – AN ELECTRON
MICROSCOPIC STUDY**

Zoltán Süle, M.Sc.

Ph.D. thesis

Experimental and Clinical Neuroscience Doctoral Programme
Doctoral School of Medicine

Supervisors:

Eszter Farkas, M.Sc., Ph.D.

Prof. András Mihály, M.D., Ph.D., D.Sc.

Department of Anatomy, Histology and Embryology
Faculty of Medicine, University of Szeged

Szeged

2010

LIST OF PUBLICATIONS, RELATED TO THIS THESIS

- I. Fabene PF, Weiczner R, Marzola P, Nicolato E, Calderan L, Andrioli A, Farkas E, **Süle Z**, Mihály A, Sbarbati A: Structural and functional MRI following 4-aminopyridine-induced seizures: a comparative imaging and anatomical study.
Neurobiol Dis. 2006 Jan; 21(1):80-9 **IF: 4.128**
- II. Farkas E, **Süle Z**, Tóth-Szűki V, Mátyás A, Antal P, Farkas IG, Mihály A, Bari F: Tumor necrosis factor-alpha increases cerebral blood flow and ultrastructural capillary damage through the release of nitric oxide in the rat brain.
Microvasc Res. 2006 Nov; 72(3):113-9 **IF: 2.477**
- III. **Süle Z**, Mracskó É, Bereczki E, Sántha M, Csont T, Ferdinándy P, Bari F, Farkas E: Capillary injury in the ischemic brain of hyperlipidemic, apolipoprotein B-100 transgenic mice.
Life Sci. 2009 Jun 19; 84(25-26):935-9 **IF: 2.560**

Cumulative Impact Factor = 10.153 (ISI JCR 2009)

LIST OF ABSTRACTS PUBLISHED IN CITED JOURNALS, RELATED TO THIS THESIS

- i. **Süle Z**, Tóth-Szűki V, Antal P, Mátyás A, Mihály A, Bari F, Farkas E: TNF- α -induced microvascular damage is mediated by nitrogen monoxide in the rat brain.
Clin.Neurosci./Ideggógy. Szle. 2006, 59 (1 klsz.) **IF: -**
- ii. **Süle Z**, Bari F, Sántha M, Bereczki E, Farkas E: Capillary injury in the ischemic brain of hyperlipidemic, apolipoprotein b-100 transgenic mice.
J. Vasc. Res., 2008, 45, (Suppl. 2), 122 **IF: 2.792**
- iii. **Süle Z**, Kovács GG, Mihály A, Farkas E: Microvascular aberrations in the white matter in Alzheimer's disease.
J. Neurol. Sci., 2009, 283, (1-2), 286 **IF: 2.324**

Cumulative Impact Factor = 5.116 (ISI JCR 2009)

LIST OF ABBREVIATIONS

1VO	one-vessel occlusion
2VO	two-vessel occlusion
a	astrocytic endfoot
A β	beta-amyloid
AD	Alzheimer's disease
ANOVA	analysis of variance
apoB-100	apolipoprotein B-100
ASC	atherosclerosis
BBB	blood-brain barrier
BM	basement membrane
CBF	cerebral blood flow
CNS	central nervous system
coll	collagen deposition
Cpu	caudate putamen
CT	computer tomography
e	endothelial cell
em	endothelial mitochondria
en	endothelial nucleus
ep	endothelial cytoplasm
er	erythrocyte
EAAT	excitatory amino acid transporter
FWM	frontal white matter
F	female
FM	focal mild
γ -GTP	gamma-glutamyl transpeptidase
GLUT-1	glucose transporter isoform-1
Gm	gray matter
HSPG	heparin sulfate proteoglycan
i.c.	intracarotid
i. m.	intramuscular
i.p	intraperitoneal
i.v.	intravenous
l	capillary lumen
p	pericyte
pn	nucleus of pericyte
LDL	low density lipoprotein
L-NAME	<i>N</i> (G)-nitro-L-arginine-methyl-ester
LS	lateral septum
LV	lateral ventricle
M	male
MRI	magnetic resonance imaging
NO	nitric-oxide
NOS	nitrogen-monoxide synthase
O	occipital
P	parietal
PD	Parkinson's disease
PWM	parietal white matter
rCBF	regional cerebral blood flow

LIST OF ABBREVIATIONS (contd.)

ROS	reactive oxygen species
SPECT	single photon emission computed tomography
Tg	transgenic
tj	tight junction
TNF α	tumor necrosis factor-alpha
VDB	ventral diagonal band
VEGF	vascular endothelial growth factor
VLDL	very low density lipoprotein
Wt	wild-type
WM	white matter
y	years

CONTENTS	Page
1. INTRODUCTION	6
1.1. General architecture of the brain capillaries in healthy conditions	6
1.2. Morphological units of the BBB	7
1.2.1. Endothelial cells	7
1.2.2. Pericytes	8
1.2.3. Astrocytes	9
1.2.4. Basement membrane	9
1.3. Ultrastructure of the blood-brain barrier in pathological conditions	10
1.4. Cerebrovascular and other risk factors for Alzheimer's disease	10
1.4.1. Cerebrovascular risk factors for AD	11
1.4.2. Effects of the neuroinflammation on AD	11
1.4.3. Effects of the hyperlipidemia on AD	12
2. OBJECTIVES	14
3. MATERIALS AND METHODS	15
3.1. Experimental models / study population	15
3.1.1. Effects of normal aging and Alzheimer's disease on cerebral white matter microvessels – a human study	15
3.1.2. Effects of circulating TNF α on blood-brain barrier ultrastructure – a rat study	16
3.1.3. Effects of hyperlipidemia and/or ischemia on blood-brain barrier ultrastructure – a mouse study	18
3.2. Electron microscopy	18
3.2.1. Sample preparation, and examination	19
3.2.2. Determination of microvascular damage and quantitative analysis	20
3.2.3. Statistical analysis	21
4. RESULTS	22
4.1. The ultrastructure of cerebral white matter microvessels in normal aging and Alzheimer's disease	22
4.2. Effects of circulating TNF α on blood-brain barrier ultrastructure	25
4.3. Effects of hyperlipidemia and/or ischemia on blood-brain barrier ultrastructure	27
5. DISCUSSION	30
5.1. Alterations of cerebral white matter microvessels in normal aging and Alzheimer's disease	31
5.1.1. Cerebral blood flow and microvascular alterations in normal aging	32
5.1.2. Cerebrovascular pathology in AD	33
5.2. BBB ultrastructure in inflammatory processes	34
5.3. The ultrastructure of the BBB in hyperlipidemia and/or ischemia	36
6. CONCLUSIONS	39
7. ACKNOWLEDGEMENTS	40
8. REFERENCES	41
9. APPENDIX	50

1. INTRODUCTION

1.1. General architecture of the brain capillaries in healthy conditions

Cerebral capillaries represent the finest branches of the vascular tree in the human brain. They form anastomoses, and create a three dimensional vascular network. The surface area of the brain microvasculature is approximately $100 \text{ cm}^2/\text{g}$ tissue; the mean intercapillary distance in the human brain is about $40 \text{ }\mu\text{m}$ (Duvernoy et al., 1983). It is a well known phenomenon, that the density and distribution of the capillaries vary in different brain areas. For example, the microvascular density in the gray matter is approximately three times higher than that of the white matter. Moreover, the functional activity and nutrient claim of the given brain region determine the distribution of its capillary network. This concept is supported by the observation, that local cerebral blood flow and capillary length per brain volume show a remarkable correlation (Gjedde and Diemer, 1985). Also, synapse-rich layers are highly vascularized, cell body populations contain less dense microvascular networks, and neural fiber bundles receive a relatively moderate blood supply. Finally, vascular distribution may be defined by the specific tasks of a brain area: the motor centers receive lower blood supply than the sensory and association centers.

The cerebral capillaries have unique ultrastructure, which forms and serves the blood-brain barrier (BBB) (Figure 1). There are three main cellular components of the BBB; the endothelial cells of the capillaries, the special connective tissue elements called pericytes, and finally the astrocytic endfeet surrounding the capillaries. The cellular units are surrounded by an accessory basement membrane. For the occlusion and the prevention of paracellular transport, in between the contact points of the adjacent endothelial cells, tight junctions (*zonulae occludentes*) appear, which form the morphological basis for BBB. The BBB is a specialized system of capillary endothelial cells that protects the brain from harmful substances in the blood stream, while supplying the brain with the required nutrients for proper function. Unlike peripheral capillaries that allow relatively free exchange of substance across / between cells, the BBB strictly limits transport into the brain through physical, metabolic and enzymatic barriers. BBB breakdown is thought to be a key component in central nervous system (CNS) associated pathologies.

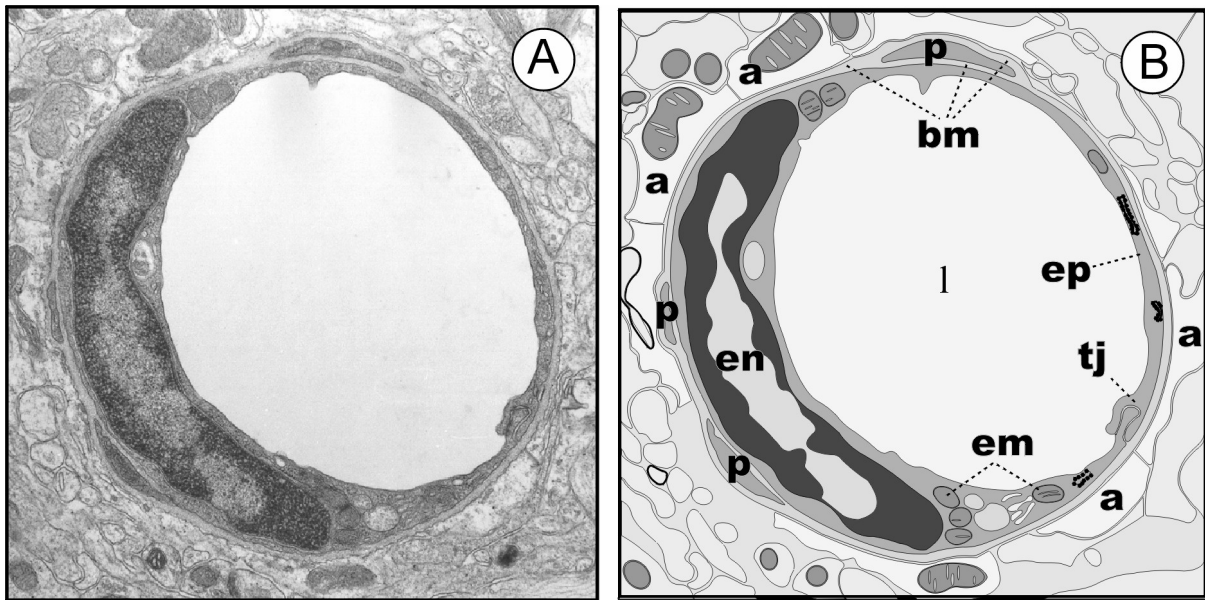


Figure 1. Ultrastructure of a cerebral capillary's cross section. A: an electron microscopic image of a typical cortical capillary from the frontoparietal cortex of a Wistar rat. B: graphic redrawn of the vessel. Abbreviations: a: astrocytic endfeet; bm: basement membrane; em: endothelial mitochondria; en: endothelial nucleus; ep: endothelial cytoplasm; l: capillary lumen; p: pericyte; tj: tight junction. (With kind permission of Eszter Farkas.)

1.2. Morphological units of the BBB

1.2.1. Endothelial cells

The endothelial cells of the BBB show some special features which are unique and set them apart from peripheral endothelial cells. Comparative morphometric analysis of the wall of a cerebral versus a muscular capillary revealed that the wall thickness of brain capillaries is almost 40% lower than that of capillaries in muscles (Coomer and Stewart, 1985). The narrower wall of the cerebral capillaries could possibly be complementary to the restrictive permeability of the BBB, allowing nutrients a shortened transport time to cross the BBB and enter the brain parenchyma. The cerebral endothelial cytoplasm contains only a few pinocytotic vesicles and the capillary wall is not fenestrated (Abbott, 2005).

There are various transport mechanisms through the BBB. Paracellular diffusion (in between the neighboring cells) is not frequent because of the tight junctions; only the water is able to traffic in this way in non-pathological conditions. The transcellular transport mechanisms make use of various energy-dependent and non energy-dependent pathways. Quantitative biochemical studies provided evidence for a functional polarity of the BBB. The luminal and abluminal membrane surfaces of the capillary endothelial cells are different

according to their specific functions (Betz and Goldstein, 1978). An electron microscopic immunogold study showed, that the concentration of the glucose transporter isoform 1 (GLUT-1), the principal glucose transporter of the BBB, is approximately 4-fold higher in the abluminal than in the luminal endothelial membrane (Farrell and Pardridge, 1991).

The number of mitochondria and their volume in BBB endothelial cells is higher as compared with the peripheral endothelial layer (Oldendorf et al., 1977), which is thought to be required for the active transport of nutrients and waste products through the BBB. The barrier function is further supported by an enzymatic barrier at the cerebral endothelial layer, capable of metabolizing drugs and nutrients (Minn et al., 1991; Brownlees and Williams 1993; Brownson et al., 1994). These enzymes are principally directed at metabolizing neuroactive blood-borne peptides. Enzymes such as γ -glutamyl transpeptidase (γ -GTP), alkaline phosphatase, and aromatic acid decarboxylase are in elevated concentration in cerebral microvessels, yet often in low concentration or absent in non-neuronal capillaries.

1.2.2. Pericytes

Pericytes in the periphery are flat, undifferentiated, contractile connective tissue cells, which surround capillary walls. The association of pericytes to blood vessels has been suggested to regulate endothelial cell proliferation, survival, migration, differentiation, and vascular branching (Hellström et al., 2001). Pericytes send out cellular projections, which penetrate the basal lamina and cover approximately 20-30% of the microvascular circumference (Frank et al., 1987). Pericytes are thought to contribute to endothelial cell proliferation via selective inhibition of endothelial cell growth (Antonelli-Orlidge et al., 1989). In support of this notion, the lack of pericytes has lead to endothelial hyperplasia and abnormal vascular morphogenesis in the brain (Hellström et al., 2001). Electrophysiological measurements have showed, that pericytes in the cerebellum and in retina are able to control the capillary diameter according to the extracellular Ca^{2+} level or presence of various vasoactive neurotransmitters, such as noradrenaline or adenosine triphosphate (Peppiatt et al., 2006).

Pericytes of the BBB might be derived from or convert to microglia, since the cerebral pericytes demonstrate the capacity to phagocytize exogenous proteins from the CNS, and display macrophage surface markers (Coomber and Stewart, 1985).

1.2.3. Astrocytes

Astrocytes are star-shaped glial cells of the CNS, which envelop more than 99% of the BBB endothelium (Hawkins and Davis, 2005). Astrocytes serve as a guiding mesh and play an active role in the induction of the BBB. Their processes terminate as endfeet at the basal lamina of the blood vessels, and form a limiting membrane (*membrana limitans gliae perivascularis*) around them.

There is significant body of evidence to indicate that astrocyte interaction with the cerebral endothelium helps determine BBB function, morphology (i.e. tightness), and protein expression (Beck et al., 1984; Arthur et al., 1987; Cancilla et al., 1983). *In vitro* cell culture models helped to clarify the astrocytic roles in this process. Cerebral microvascular endothelial cells in themselves were able to form a BBB-like phenotype but with loss of some important functions (leakier tight junctions, downregulated transport and enzyme systems) (Krämer et al., 2001). Some of those properties can be reconditioned in experimental models, which are based on cerebral endothelial cells co-cultured with astrocytic cell lines. Rubin et al. (1991) clearly demonstrated that the tight junctional proteins are upregulated by astrocytes. Even more interesting is that astrocytes have the ability for the induction of BBB markers on peripheral endothelial cells (Kuchler-Bopp et al., 1999).

In addition to the constitution of the BBB, another most important function of the mature astrocytes is the regulation of cerebral blood flow (CBF) and vascular tone, which is based on the expression and function of serotonergic and cholinergic receptors on the perivascular endfeet (Luiten et al., 1996; Elhousseiny et al., 1999; Cohen et al., 1997).

1.2.4. Basement membrane

A well-defined basement membrane (BM) covering the endothelial cells and embracing pericytes supports the cerebral capillary walls. The BM is composed of three different sublayers: a *lamina rara interna* along the abluminal endothelial surface, a middle layer called *lamina densa*, and an outmost *lamina rara externa* medial to the astrocytic endfeet. The average thickness of the cerebral capillary BM is about 30-40 nm. The BM constitutes of extracellular matrix components such as type IV collagen, heparan sulfate proteoglycan (HSPG), tenascin, laminin and extrinsic fibronectin. The major structural element of the BM is type IV collagen, which is preferentially located in the *lamina densa*, while the proteins laminin and HSPG are more closely associated with the two *lamina rarae*. Cell adhesion to

the basal lamina relies on integrins, which are transmembrane receptors that bridge the cytoskeletal elements of a cell to the extracellular matrix. The BM provides mechanical support for cell attachment, serves as a substratum for cell migration, separates adjacent tissue, and can act as a barrier to the passage of macromolecules.

1.3. Ultrastructure of the blood-brain barrier in pathological conditions

The morphological features of brain capillaries can be best studied with electron microscopy. Under various pathological conditions, the cerebral capillaries display typical malformations. In aging, or cerebral ischemia, the apical surface of the endothelial cells appear irregular, display microvillus-like processes into the lumen, and empty vacuoles may form occasionally (Oomen et al., 2009; Süle et al., 2009). Pericytes often show type IV collagen and dense body (lysosomes) accumulation in their cytoplasm (Farkas et al., 2000). Damage or disruption of the BBB causes swelling of the astrocytic endfeet, which typically appears as hypodense pericapillary areas in electron microscopic images. The most common ultrastructural deviations of the basement membrane concern the accumulation of extracellular matrix proteins, which results in BM thickening and/or fibrous collagen deposition.

1.4. Cerebrovascular and other risk factors for Alzheimer's disease

Sporadic (i.e. not genetically inherited) AD is considered as a multifactorial, progressive neurodegenerative disorder. In addition to amyloid toxicity and defect in tau-phosphorylation, various risk factors, such as cerebral hypoperfusion, neuroinflammation and hypercholesterolemia contribute to the development of AD (Fig. 2).

1.4.1. Cerebrovascular risk factors for AD

Vascular risk factors are considered as major contributors to disease evolution and progression in AD. As such, moderate but persistent reduction in regional CBF compromises memory processes and contributes to the development and progression of dementia (Farkas et al., 2007). The association of decreased CBF (particularly in the temporal and parietal cortices) with AD has been firmly established (de la Torre, 2002; Farkas and Luiten, 2001; Matsuda, 2001), and the degree or pattern of cerebral hypoperfusion in mild cognitive

impairment has been proposed as a predictive marker for the progression to AD (Borroni et al., 2006; Hirao et al., 2005).

Persistently low baseline CBF has been proposed to induce ultrastructural pathology of the cerebral microvessels (Farkas and Luiten, 2001) (Fig. 2). The BBB displays hypoperfusion-related ultrastructural abnormalities in the form of BM thickening and fibrous collagen deposits, which develop chronically during aging and dementia (Farkas and Luiten, 2001). The accumulation of collagen fibers in the microvascular BM may hinder specific BBB transport for important nutrients such as glucose and essential amino acids (Farkas and Luiten, 2001). In the aging brain, a significant correlation has been established between collagen deposits in the microvascular wall and advancing age in the frontal and occipital white matter (Farkas et al., 2006). Further, in AD, the proportion of capillaries displaying collagen accumulation in the microvascular BM in the cingulate cortex was considerably higher than in age-matched controls (Farkas et al., 2000). Whether such BM pathology is related to cerebral hypoperfusion has been tested in rats, of which the common carotid arteries were permanently occluded (2-vessel occlusion, 2VO). Electron microscopic examination revealed microvascular BM thickening and collagen deposits 14 months after 2VO onset, which were comparable to those seen in the human post mortem studies. The proportion of affected capillaries in the hippocampus in 2VO rats was almost twice that in the controls (De Jong et al., 1999). Based on the above findings, chronic cerebral hypoperfusion is suggested to be a causative, accelerating condition for ultrastructural BBB damage, which is also the focus of our current investigation.

The cause for cerebral hypoperfusion in AD has not been unequivocally defined; a number of competing and complementary hypotheses exist. The development of atherosclerotic plaques in the carotid arteries or any other cerebral resistance vessels narrows the vascular lumen and renders the vessel wall too rigid for the fine regulation of vascular diameter, thereby compromising optimal blood supply to the brain. Indeed, clinical studies have demonstrated a link between carotid intima-media thickness and cognitive decline (Silvestrini et al., 2009), and the association between atherosclerosis in the carotid arteries and a higher risk for AD (van Oijen et al., 2007).

1.4.2. Effects of the neuroinflammation on AD

Inflammation has also been proposed to be involved in the pathogenesis of AD. For instance, the expression of an innate pro-inflammatory cytokine profile in middle age

appeared as an early risk factor of AD in old age (van Exel et al., 2009). According to a widely held view, beta-amyloid ($A\beta$) deposits in the brain parenchyma activate microglia, which, in turn release pro-inflammatory cytokines and reactive oxygen species (ROS). This chronic cascade may eventually lead to neuronal damage (Neuroinflammation Working Group, 2000). While inflammation within the brain is thus thought to be a potentially major neurodegenerative process, links between AD and inflammation in the periphery have also been suggested (McNaull et al., 2010). As such, peripheral blood mononuclear cells produce higher levels of pro-inflammatory cytokines upon stimulation in mild cognitive impairment and early AD (Magaki et al., 2007). However, no association between circulating inflammatory mediators and cerebrovascular injury that occurs in AD has been investigated. Here we set out to characterize ultrastructural BBB damage after intracarotid infusion of the pro-inflammatory cytokine, tumor necrosis factor- α (TNF α) in the rat, and to define whether nitric oxide (NO) is a mediator of TNF α in this regard.

1.4.3. Effects of the hyperlipidemia on AD

High plasma lipid content is known to favor plaque formation. Incidentally, high dietary cholesterol intake increases, while the use of statins reduces the risk for AD (Sparks, 2008; Sparks et al., 2008). Hypercholesterolemia caused by elevated plasma concentration or abnormal metabolism of low density lipoprotein (LDL, an important carrier of cholesterol), accelerates atherosclerosis (Grundy et al., 1985; Rudel et al., 1986). Furthermore, recent evidence suggests that the triglyceride-rich very low density lipoprotein (VLDL) also contributes to atherogenesis possibly through the inflammatory activation of vascular or foam cells (Libby, 2007; Persson et al., 2006). Apolipoprotein B-100 (apoB-100) is a constant surface component of both the cholesterol carrier LDL, and the triglyceride-rich VLDL in circulating blood plasma. It plays a pivotal role in VLDL assembly in the liver, and binds to specific receptors on the cell membranes to direct the lipoproteins to their proper metabolic sites (Blasiolo et al., 2007; Olofsson and Boren, 2005). In atherogenesis, apoB-100 assembles atherogenic lipoproteins and acts as a mediator in the interaction between LDL and proteoglycans in the vascular wall, thereby promoting lipoprotein retention in the vascular intima. The elevated production or decreased removal of apoB-100-containing LDL from plasma has been associated with an increased susceptibility for atherosclerosis (Grundy et al., 1985). In AD, apoB-100 was found up-regulated in the serum as shown by a proteomics study surveying potential plasma biomarkers for AD (Song et al., 2009).

Genetically engineered mice expressing human apoB-100 (Tg(*apoB-100*)) were generated in order to model hyperlipidemia with increased serum cholesterol or triglyceride concentrations similar to human conditions (Chiesa et al., 1993; Csont et al., 2007; Linton et al., 1993), and to investigate related cardiovascular pathologies in experimental models (Csont et al., 2007; Purcell-Huynh et al., 1995). The established cardiovascular pathology of Tg(*apoB-100*) mice prompted us to explore potential, ultrastructural microvascular abnormalities in their brains, which may be relevant for the evolution of cerebrovascular injury AD.

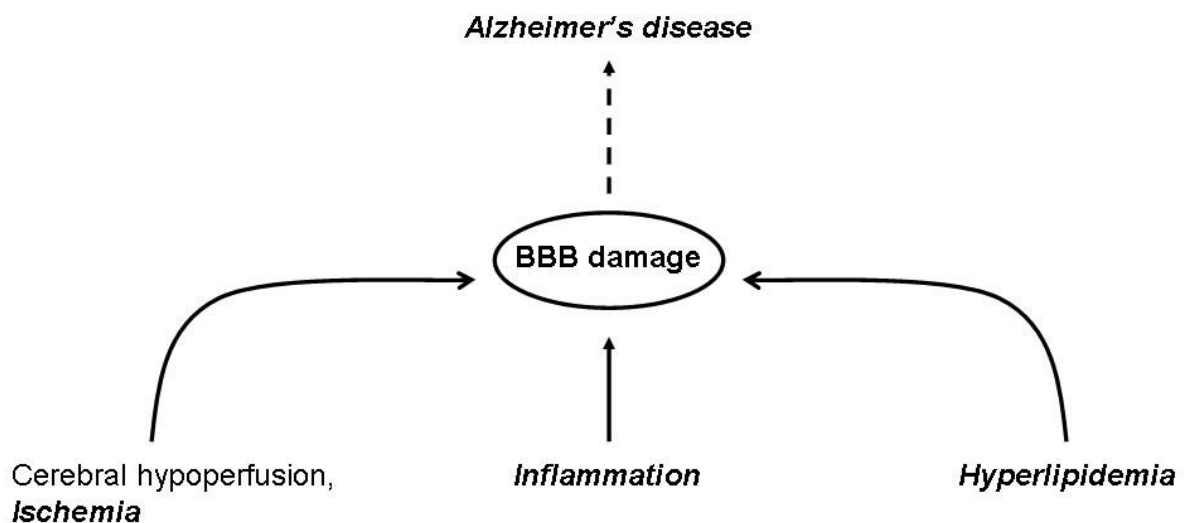


Figure 2. Various risk factors, considered in this study, which are expected to cause blood-brain barrier (BBB) damage that may contribute to Alzheimer's disease. The focus of our investigations was the ultrastructural malformations of the BBB. Conditions that were investigated in various experimental paradigms are highlighted in *italics*.

2. OBJECTIVES

The general aim of our study was to describe the possible ultrastructural aberrations of the cerebral microvasculature in various pathological conditions. The disease processes specified below all occur – alone or in combination - in AD with ischemic components.

First, we sought to determine whether:

- a) the microvasculature of the cerebral periventricular white matter is injured in Alzheimer's disease;
- b) the potential microvascular damage affects all white matter areas (i.e. frontal, parietal, occipital) equally.

Second, we set out to:

- a) investigate the effect of systemic inflammation (e.g. high level of the circulating proinflammatory cytokine TNF α) on the ultrastructure of the blood-brain barrier;
- b) determine whether NO is a mediator of the expected TNF α -induced alterations in blood-brain barrier ultrastructure.

Third, we aimed to investigate whether hyperlipidemia:

- a) causes cerebral microvascular lesions in itself;
- b) augments ischemia-related capillary damage.

3. MATERIALS AND METHODS

3.1. Experimental models / study population

All animal experiments were approved by the Ethical Committee of the University of Szeged. In the human study, samples were collected based on informed consent, approved by the Regional Ethics Committee for Human Medical Biology Research of the University of Szeged.

3.1.1. Effects of normal aging and Alzheimer's disease on cerebral white matter microvessels – a human study

Sampling: Post mortem periventricular white matter samples of 17 patients were collected at autopsy from the frontal, parietal and occipital lobes (Fig. 3A), and kindly provided by Dr. Géza G. Kovács (now at: Institute of Neurology, Medical University Vienna, Vienna, Austria). The tissue blocks (1x1x1 cm) were immersed in Karnovsky fixative (2.5% glutaraldehyde and 2% paraformaldehyde in 0.1 M phosphate buffer, pH 7.4) and stored in the same solution until further processing.

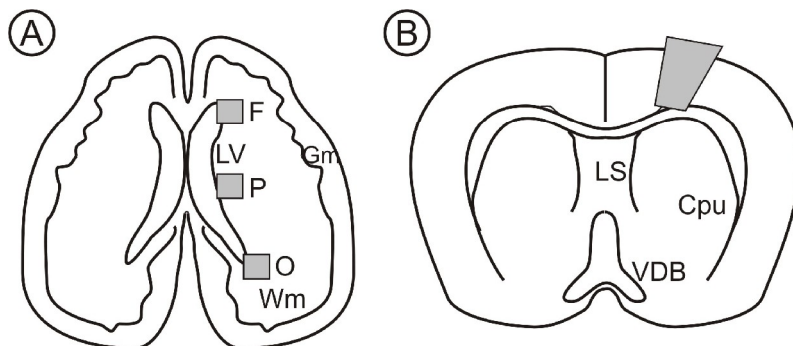


Figure 3. Sites of sampling.

A: human, horizontal plane. B: rodent, frontal plane (Bregma 1.34; Paxinos and Watson, 1986).

Abbreviations: Cpu: caudate putamen, F: frontal, Gm: grey matter, LS: lateral septum, LV: lateral ventricle, O: occipital, P: parietal, VDB: ventral diagonal band, Wm: white matter.

Characterization of cases: Table 1 presents the pathological characterization of the subjects, obtained from the neuropathologist's data base. The age of the mixed study group of males and females ranged between 69 and 95 years (81 ± 1.5 years). The post-mortem time (10 ± 1.9 hours) was within a day except for one case (32 h). The neuropathological evaluation focused on the Braak staging indicative of the progression of Alzheimer's disease, and cortical Lewy body pathology also associated with dementia. Focal, mild atherosclerosis in the circle of Willis was labeled when yellow small plaques appeared in the vascular wall. Peripheral vascular risk factors have been also assessed. The degree of peripheral atherosclerosis was determined by examining the aorta, the carotid bifurcation and coronary

arteries. The semi-quantitative evaluation reflected the expansion of the affected areas. Atherosclerosis was evaluated as mild (+) in case only the coronary arteries were affected. Severe peripheral atherosclerosis (++) was noted when – in addition to the coronary arteries - a number of vessels including the carotid arteries appeared sclerotic.

Case no.	Age (y)	Gender	Post mortem time (h)	Neuropathology		Vascular risk factors		
				Braak stage	Lewy body pathology	ASC in the circle of Willis	Peripheral ASC	Hypertension
1	95	M	11	IV	Limbic	No	+	+
2	84	F	5	V	-	FM	+	+
3	80	M	6	VI	-	FM	++	-
4	88	F	32	II	-	No	+	+
5	79	F	7	II	-	FM	++	+
6	85	F	5	III	-	No	-	+
7	81	F	5	IV	Neocortical	No	-	-
8	74	F	4	IV	Neocortical	No	++	+
9	86	F	13	III	-	No	-	+
10	81	F	5	-	-	No	-	-
11	85	F	12	IV	Limbic	FM	++	+
12	69	M	9	I	-	No	+	+
13	76	M	23	-	-	No	-	+
14	83	F	4	-	-	No	++	+
15	83	M	20	-	-	No	++	-
16	72	M	8	-	-	FM	-	-
17	78	F	5	VI	Limbic	FM	++	+

Table 1. Characterization of the study population. Abbreviations: ASC: atherosclerosis, F: female, FM: focal mild, M: male, y: years

3.1.2. Effects of circulating TNF α on blood-brain barrier ultrastructure – a rat study

Surgical procedure: Fifty male Wistar rats (280-350g) were anesthetized with 5% chloral hydrate (40 mg/kg i.p.); anesthesia was maintained continuously up to the end of the experiment. Body temperature was kept at 37°C with a heating pad. The trachea was intubated, and the animals were artificially ventilated with a small pet respirator (SAR-830/P CWE Inc. U.S.A.). The right femoral vein and the right common carotid artery were cannulated for the infusion of solutions.

Application of solutions: Animals were pretreated (n=30) or not (n=20) with the nitrogen monoxide synthase (NOS) inhibitor *N*(G)-nitro-L-arginine-methyl-ester (L-NAME), at a dose of 20 mg/kg in 1 ml saline, given over 2 minutes intravenously. Fifteen minutes after the L-NAME infusion, TNF α (2.5 μ g/kg, solubilized in 1 ml phosphate-buffered saline; human recombinant, Sigma) or 1 ml saline was administrated at a speed of 0.1 ml/min into the right common carotid artery with a laboratory pump. The combination of treatments and various survival times are presented in Table 2.

Solutions		n	Survival time
Saline/TNF α , i.c.	L-NAME, i.v.		
Saline	-	5	45 min
	+	5	
TNF α	-	5	
	+	5	
Saline	+	5	4 h
	-	5	
TNF α	+	5	
	-	5	
Saline	+	5	8 h
	-	5	
TNF α	-	5	
	+	5	

Table 2. The composition of the various experimental groups. Abbreviations: i.c.: intracarotid, i. v.: intravenous, L-NAME: *N*(G)-nitro-L-arginine-methyl-ester, TNF α : tumor necrosis factor-alpha

Sampling: The animals were sacrificed by transcardial perfusion with saline followed by a solution of 2.5% glutaraldehyde and 2% paraformaldehyde in 0.1M phosphate buffer, 45 min, 4 h or 8 h after the end of TNF α or saline infusion. The brains were removed and stored in the same solution until further processing. Samples of the ipsilateral, frontoparietal cortex (Bregma 0.20 mm; Paxinos and Watson, 1986) (Fig. 3B) were prepared for electron microscopy.

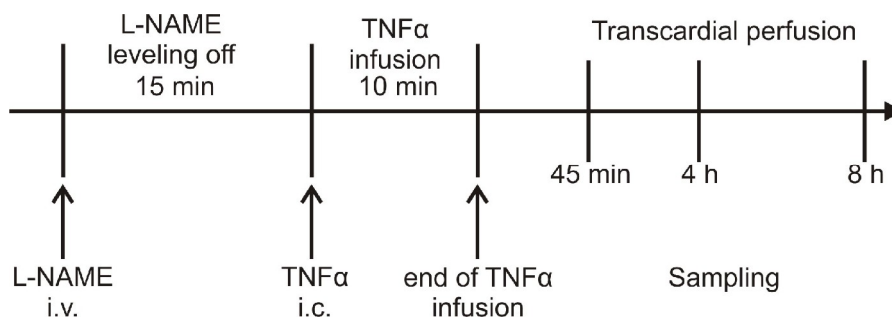


Figure 4. Experimental protocol. Abbreviations: i.c.: intracarotid, i.v.: intravenous, L-NAME: *N*(G)-nitro-L-arginine-methyl-ester, TNF α : tumor necrosis factor-alpha

3.1.3. Effects of hyperlipidemia and/or ischemia on blood-brain barrier ultrastructure – a mouse study

Transgenic model and dietary regime: Transgenic and wild-type mice were generated, raised, characterized (i.e. serum lipid profile), and kindly supplied by the research group of Miklós Sántha (Laboratory of Animal Genetics and Molecular Neurobiology, Institute of Biochemistry, Biological Research Center, Szeged) and Tamás Csont (Cardiovascular Research Group, Department of Biochemistry, Faculty of Medicine, University of Szeged). Transgenic mice expressing human apolipoprotein B-100 (Tg(apoB-100)) were generated as previously described (Bjelik et al., 2007; Csont et al., 2007). Six-week-old Tg(apo-b 100) (n=23) and wild-type (Wt) mice (C5/B6, n=26) were fed for 17-19 weeks with standard laboratory rodent chow (Szinbad Ltd., Hungary), or 2% cholesterol-enriched diet prepared by supplementing the standard diet with cholesterol. The animals received food *ad libitum* throughout the study; the body weight at the end of the dietary regime was similar for all experimental groups (Table 3). Serum lipid levels were determined in blood samples to justify the development of hyperlipidemia (Csont et al., 2007). Table 3 gives a summary of the composition, body weight and serum lipid concentration for the different experimental groups.

Experimental groups		n male/female	Body weight g mean±SEM	Serum lipid levels		
Genotype	Diet			Total cholesterol (mmol/L)	LDL cholesterol (mmol/L)	Triglycerides (mmol/L)
Wild-type		13 (7/6)	28±1.3	2.54±0.17	1.14±0.10	0.99±0.13
Tg(apoB-100)	Standard	11 (4/7)	27±1.5	2.68±0.11	1.09±0.12	1.63±0.20*
Wild-type		13 (6/7)	28±1.9	2.70±0.24	1.37±0.13	0.78±0.11
Tg(apoB-100)	Cholesterol-enriched	12 (6/6)	27±1.0	3.51±0.33*	1.87±0.19*	0.79±0.19

Table 3. Composition of experimental groups, body weight, and serum lipid concentration in wild-type or apoB-100 transgenic mice, on standard or cholesterol-enriched diet. Data are given as mean±SEM., n=6, p* $<$ 0.05 vs. all other groups. Abbreviation: Tg(apoB-100): human apolipoprotein B-100 expressing transgenic.

Surgical procedure: The mice were anesthetized with 3% chloral hydrate (0.015 ml/g i.p.) and injected with 0.05 ml atropine (0.1 mg/ml; i.m.) at 24 weeks of age. On all of the animals, unilateral global forebrain ischemia was induced by permanent occlusion of either common carotid artery (one-vessel occlusion, 1VO). The unilateral common carotid artery was exposed via a central cervical incision, carefully separated from its connective tissue sheets and neighboring nerves and ligated with surgical silk. Finally, the wound was closed with surgical silk sutures. The reasons for the choice of the 1VO are the following: the 1VO surgical procedure in mice has been previously demonstrated to inflict both functional (behavioral) and histological correlates of cerebral ischemia (Plaschke et al., 2008; Yoshizaki et al., 2008), and our previous observations affirmed, that bilateral common carotid artery occlusion was lethal for wild-type CFLP in mice.

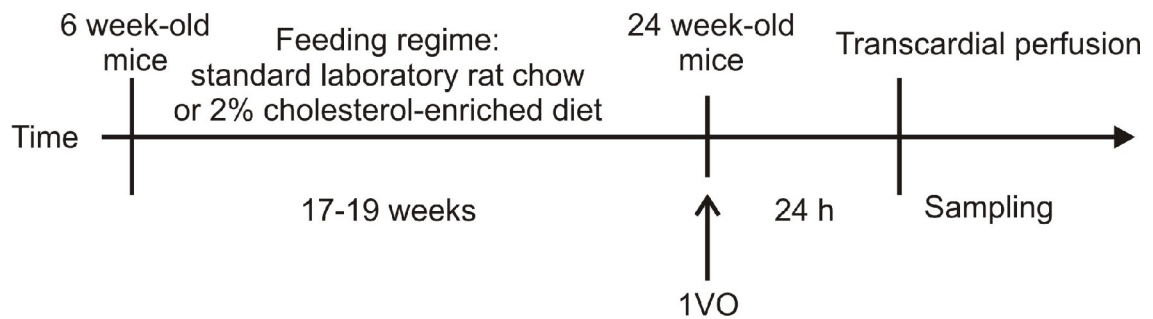


Figure 5. Experimental protocol. Abbreviation: 1VO: one-vessel occlusion

Sampling: The mice were transcardially perfused 24 h after the onset of 1VO with 50 ml 4% paraformaldehyde in 0.1 M phosphate buffer (pH=7.4) and the brains were removed. The rostral forebrains including the frontoparietal cortex were postfixed in 2.5% glutaraldehyde and 2% paraformaldehyde in 0.1 M phosphate buffer for 1 week. Samples of the ipsilateral and contralateral frontoparietal cortices (Bregma 1.34; Franklin and Paxinos, 1997) (Fig. 3B) were dissected and routinely embedded for electron microscopic investigations as described below.

3.2. Electron microscopy

3.2.1. Sample preparation, and examination

Tissue blocks were prepared for light and electron microscopic examination (Farkas et al., 2003). Samples were dehydrated by increasing concentrations of ethanol, and embedded in

Durcupan epoxy resin (Fluka). Semi-thin sections were cut on an ultramicrotome (Ultracut E, Reichert-Jung) and stained on object glasses with a 1:1 mixture of 1% methylene blue and 1% Azure II blue. The samples were then coverslipped with DPX and analyzed under a light microscope (Nikon E600). Ultrathin sections were cut from the same blocks and collected in 200-mesh copper grids. The preparations were then contrasted with 5% uranyl acetate and Reynolds lead citrate solution. Finally, the samples were analyzed with a Philips TM10 transmission electron microscope. Photographs were taken with a computer-assisted digital camera (MegaView II, Soft Imaging Systems, Germany).

3.2.2. Determination of microvascular damage and quantitative analysis

All cortical layers were systematically scanned in the rodent experiments (rat: approximately 0.13 mm² tissue surface ~25±7 capillary cross sections; mice: about 0.14 mm² cortical area ~ 28±8 capillaries), and an entire section in the human study (approximately 0.49 mm² of sample surface ~8±4 microvessels) on a randomly selected sample grid.

First, the lumen diameter of microvessels was measured. Microvessels only of a defined lumen diameter were included in the analysis (i.e. rodent: d<7mm, human d<12 mm). In case the vessel profile was not an exact cross section (circle) but slightly oval, the shortest diameter was taken. The diameters of all the investigated vessels in each sample were averaged, and this mean was used as a single value for further statistical analysis.

Vascular density was calculated for a standard surface area with the help of the sample grid as follows. The number of encountered microvascular profiles was divided by the examined surface area, which was determined by counting the number of grid squares of a standard size provided by the distributor. Vascular density was then expressed as the number of microvascular profiles on 1mm² surface.

Analysis of the changed cellular elements and the BM:

In the rodent studies, capillaries displaying finger-like endothelial processes protruding the vessel lumen (microvilli) or swollen astrocytic endfeet were counted and the number was expressed as percentage of the total number of capillaries examined. The ratio of intact capillaries (devoid of all the above pathology) was also calculated and expressed as percentage.

In the human study, the analysis focused on BM pathology, which was noted when fibrous collagen deposition in the BM occurred. This was recognized as fiber bundles in lateral view,

displaying a 64 nm periodicity typical of collagen type I, or as tightly packed circles within the BM in cross sectional view. Another investigated pathological feature was the accumulation of fibrous collagen in the pericytes surrounding the blood vessels. The number of small vessels with either of the above BM pathology was counted and expressed as percentage of the total number of microvessels examined.

The mean lumen diameters and the ratio of microvessels displaying deposited fibrous collagen in their pericytes were correlated with the progression of Alzheimer's neuropathology defined with Braak stages, and were compared with the age of the subjects'.

3.2.3. Statistical analysis

In the rat study, a two-way ANOVA paradigm of the software SPSS 12.0 was used (variables: treatment and survival time). In the mouse study, data were analyzed with a three-way ANOVA for genotype (Tg(apoB-100) vs. Wt), diet (cholesterol-enriched vs. standard) and ischemia (ipsilateral vs. contralateral cortex). In both rodent experiments, ANOVA was followed by a Fisher least significant difference (LSD) post-hoc test for group comparisons. In the human study, statistical analysis was performed with the non-parametric Mann-Whitney U-test, and correlation analysis was performed with a Pearson's one-tailed correlation test. Results were considered to be significantly different at a probability level of $p < 0.05^*$ and $p < 0.01^{**}$.

4. RESULTS

4.1. The ultrastructure of cerebral white matter microvessels in normal aging and Alzheimer's disease

In all study groups, massive fibrous collagen deposition was observed around some microvessels, either associated with the basement membrane, or incorporated into the pericytic cytoplasm (Fig. 6B, C). In healthy age-matched controls, only about 20% of the investigated vessels displayed perivascular collagen deposition; most microvessels and their outskirts were devoid of fibrous collagen bundles (Fig. 6A). In contrast, the ratio of affected microvessels increased with the progression of Braak neuropathology, particularly in the frontal and parietal white matter (FWM and PWM, respectively): the values increased from 20% to 71% in the FWM, and from 19% to 67% in the PWM (Fig. 6D). In order to evaluate the contribution of aging to BM pathology, collagen deposition in the pericytes was related to age. Increasingly more microvessels displayed perivascular collagen bundles with advancing age in the FWM, but not in the PWM (Fig. 6E).

The average microvascular lumen diameter was calculated to be 5 μm in healthy age-matched controls and in the early stages of Braak neuropathology (Fig. 7A, C). The lumen diameter increased to an average of 6.6 μm in the PWM of cases with Braak stage III-IV, and V-VI (Fig. 7A, C). In addition, a positive, linear correlation appeared between lumen diameter and age in the PWM (Fig. 7B).

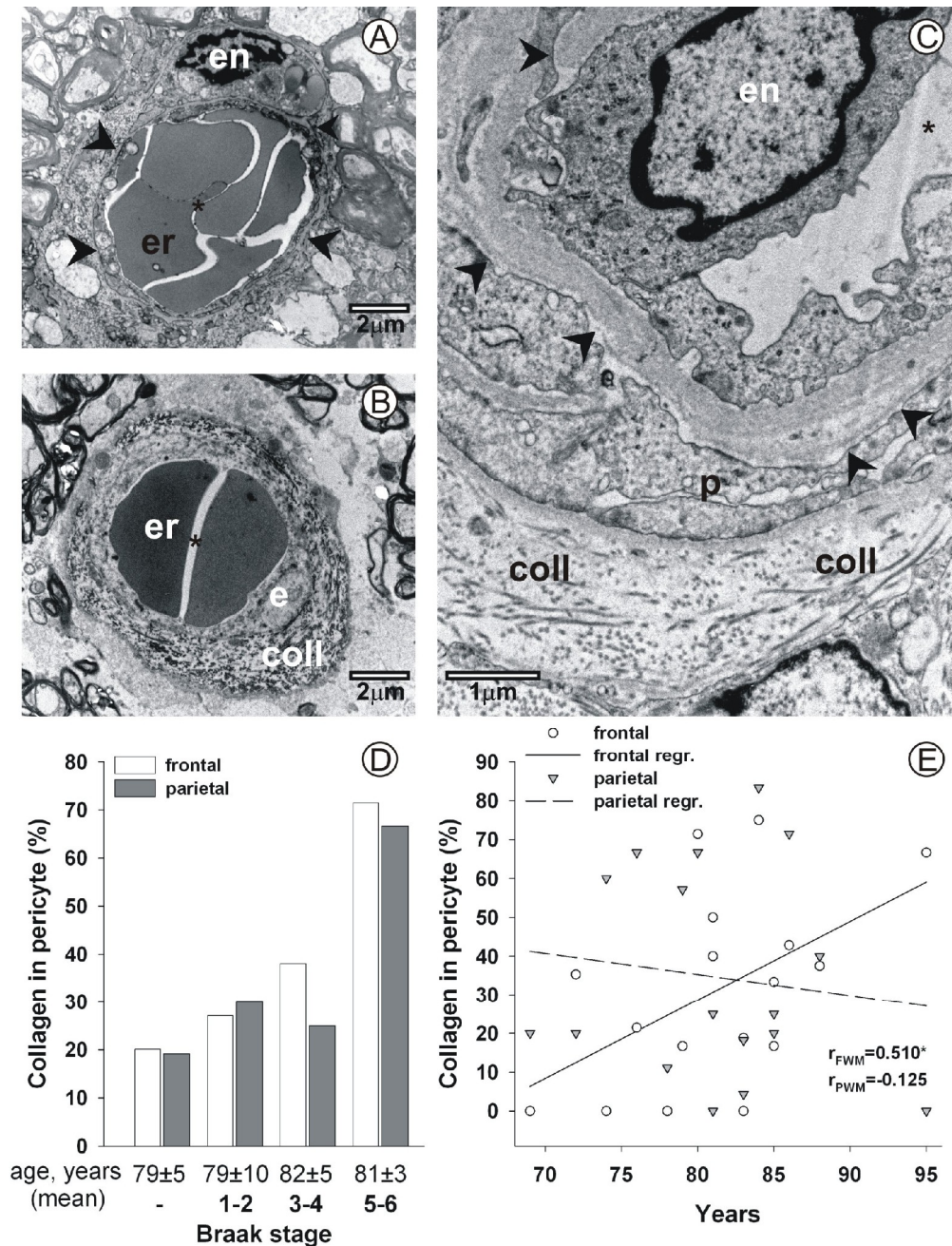


Figure 6. Ultrastructural analysis of microvessels in the frontal and parietal periventricular white matter. The photographs are representative electron microscopic images of an intact vessel profile (A; 81 years, Braak -), deposition of collagen in the vascular wall (B; 80 years, Braak IV) and fibrous collagen in the pericyte (C; 95 years, Braak IV). The bar chart in D demonstrates the increasing ratio of fibrous collagen deposited in pericytes with the progression of Alzheimer's neuropathology defined with the Braak scaling. Data in D are given as median. The graph in E demonstrates correlation analysis between the ratio of fibrous collagen deposited in pericytes (y axis) with the age of the patients (x axis). Statistical analysis was performed with a Pearson's one-tailed correlation test. The significance value is defined as $P < 0.05^*$. Abbreviations: arrowhead: basal lamina, asterisk: microvascular lumen, coll: collagen deposition, e: endothelial cell, en: nucleus of endothelial cell, er: erythrocyte, FWM: frontal periventricular white matter, p: pericyte PWM: parietal periventricular white matter.

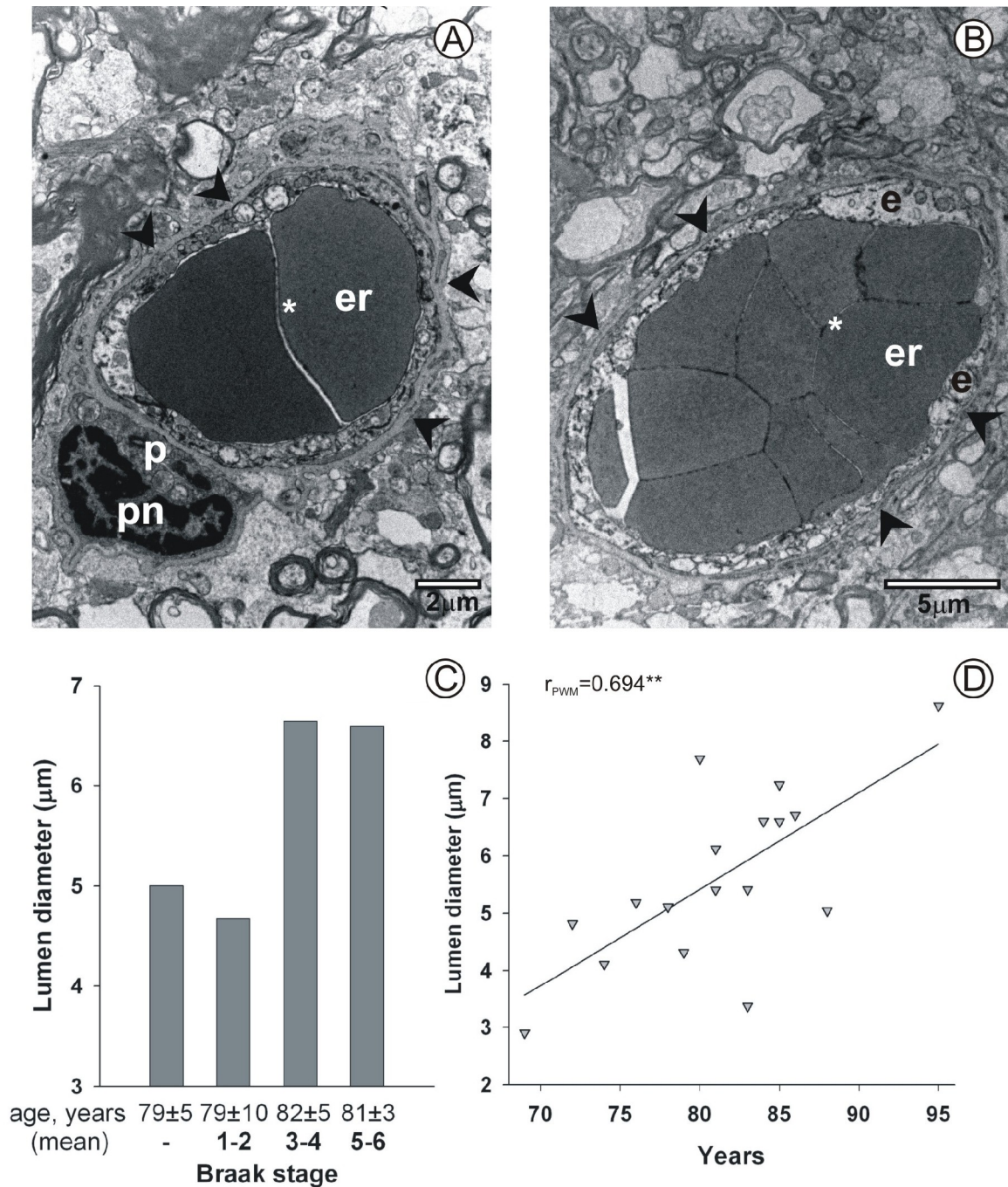


Figure 7. Lumen diameter of microvessels in the parietal periventricular white matter. Representative photographs show the microvascular lumen diameter in a control case (A; 88 years, Braak -) and a case of mild Alzheimer's neuropathology (B; 85 years, Braak III). The graph in C demonstrates microvascular lumen diameter increasing with the progression of Alzheimer's neuropathology defined with Braak scaling. Data in C are given as median. The graph in D demonstrates correlation analysis between microvascular lumen diameter (y axis) with the age of the patients (x axis). Statistical analysis was performed with a Pearson's one-tailed correlation test. The significance value is defined as $P < 0.01^{**}$. Abbreviations: arrowhead: basal lamina, asterisk: microvascular lumen, e: endothelial cell, er: erythrocyte, p: pericyte, pn: nucleus of pericyte

4.2. Effects of circulating TNF α on blood-brain barrier ultrastructure

In the semithin sections, perivascular edema was apparent around the arterioles in the brain parenchyma of the TNF α treated animals. At electron microscopic level, the endothelial cells of cerebral microvessels exhibited the following discernible abnormalities: (i) the apical surface of the endothelial cells displayed finger-like projections protruding into the lumen, and (ii) the endothelial cytoplasm contained hypodense vacuoles (Fig. 8B). The astrocytic endfeet surrounding the microvessels were swollen as shown by their low electron density and enlarged area covered (Fig. 8B-E). Around some vessels, membranous inclusions appeared in the astrocytic cytoplasm. Finally, the extensive swelling of the astrocytic endfeet occasionally deformed the capillary lumen, normally spherical in cross section (Fig. 8D).

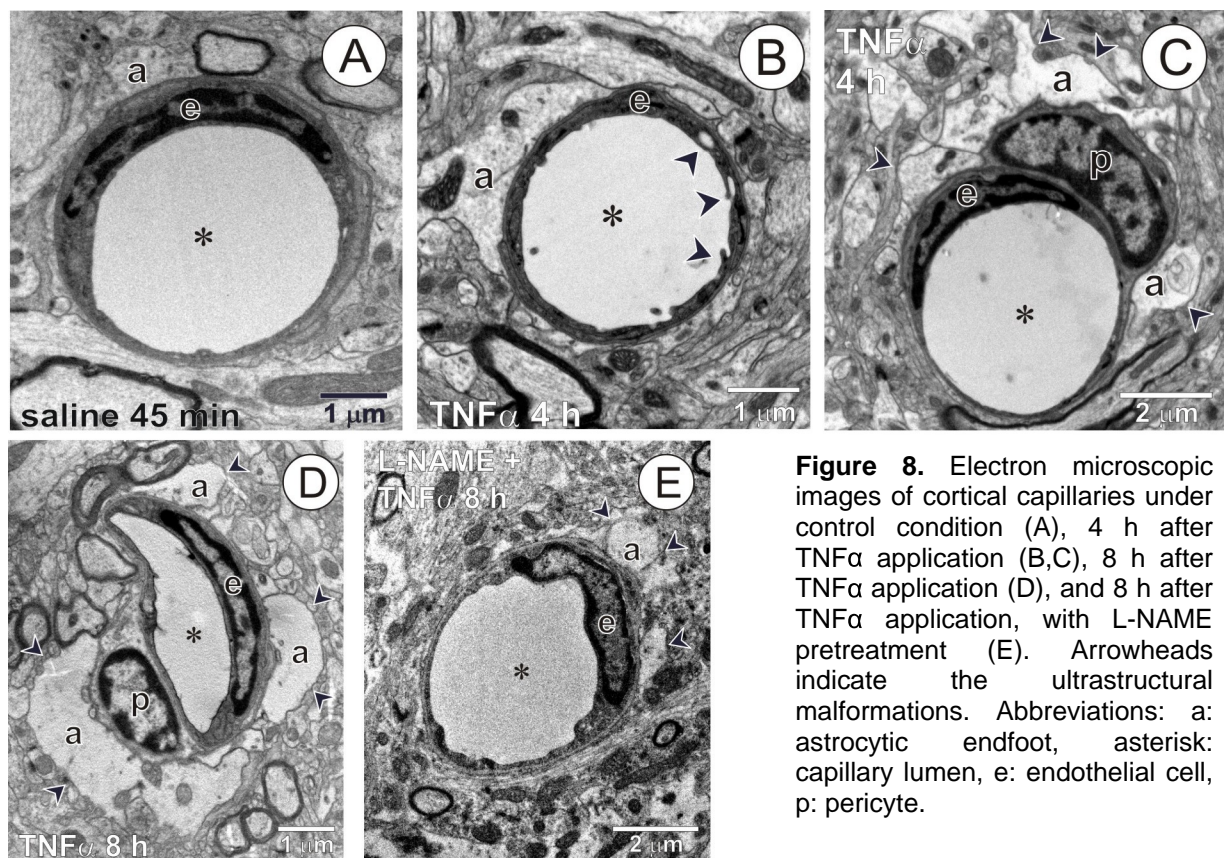


Figure 8. Electron microscopic images of cortical capillaries under control condition (A), 4 h after TNF α application (B,C), 8 h after TNF α application (D), and 8 h after TNF α application, with L-NAME pretreatment (E). Arrowheads indicate the ultrastructural malformations. Abbreviations: a: astrocytic endfoot, asterisk: capillary lumen, e: endothelial cell, p: pericyte.

According to the outcome of the quantitative analysis, TNF α infusion itself increased the ratio of capillaries with swelling of the astrocytic endfeet more than twofold at 45 min, compared to the control (48% and 22%, respectively), and a further TNF α -related increase was observed as time progressed (65% at 8 h) (Fig. 9A). In contrast, the ratio of capillaries with astrocytic swelling was reduced remarkably by L-NAME pretreatment, from 48% to 18%

at 45 min, from 61% to 34% at 4 h, and from 65% to 51% at 8 h after TNF α infusion (Fig. 9A).

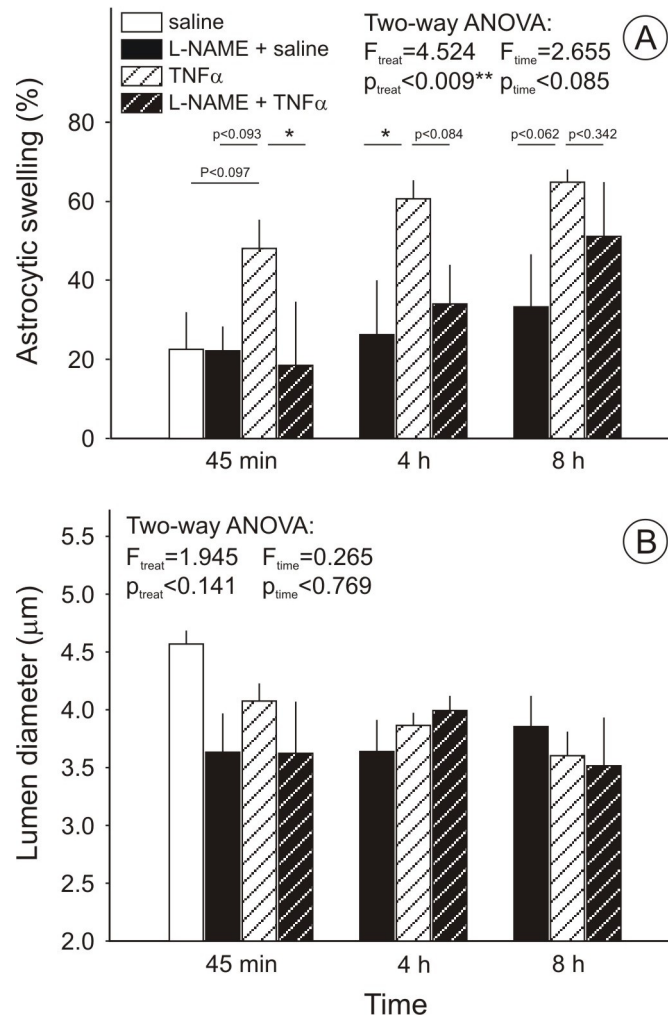


Figure 9. Quantitative data of pericapillary astrocytic swelling (A), and lumen diameter of capillaries (B). Statistical analysis was performed with an ANOVA model for two variables (treatment, survival time). Data are given as mean \pm SEM. Significance values are defined as $P<0.05^*$.

Although the statistical analysis has not revealed any significant changes in the lumen diameter of capillaries between experimental groups, both TNF α and L-NAME reduced microvascular diameter noticeably (Fig. 9B). In particular, TNF α alone reduced the lumen diameter from the control value of 4.56 μm to 4.08 μm at 45 min, which progressively decreased to 3.86 μm at 4 h, and to 3.61 μm at 8 h (Fig. 9B, white dashed bars). After the treatment with L-NAME alone or in combination with TNF α , the capillary lumen diameter varied in the interval 3.51-3.99 μm irrespective of survival time, in contrast with the 4.56 μm for the saline control group (Fig. 9B, black dashed bars).

4.3. Effects of hyperlipidemia and/or ischemia on blood-brain barrier ultrastructure

Forebrain ischemia induced in the ipsilateral frontoparietal cortex with respect to 1VO markedly increased the ratio of cortical capillaries with pericapillary astrocytic swelling from $36.5\pm 4.0\%$ to $62.1\pm 4.2\%$ in Wt mice (dietary groups merged for values, contralateral vs. ipsilateral, respectively; $P<0.001$) and from $33.2\pm 4.6\%$ to $56.0\pm 5.4\%$ in Tg(apoB-100) mice (dietary groups merged for values, contralateral vs. ipsilateral, respectively; $P<0.003$; Fig. 10C).

The luminal endothelial surface appeared to be irregular, displaying microvilli, indentations, and occasional vacuoles (Fig. 10F). The ratio of microvessels displaying endothelial microvilli demonstrated no definite change, though a slight increase appeared in the ipsilateral cortex after 1VO when compared to the contralateral side (dietary groups merged for values: 20.1 ± 2.3 vs. $14.3\pm 1.6\%$ in the Wt mice; 13.6 ± 2.7 vs. $11.7\pm 1.7\%$ in Tg(apoB-100) mice, ipsilateral vs. contralateral, respectively; Fig. 10E). The ratio of capillaries devoid of any of the above pathology (intact microvessels) decreased from an average of $65.2\pm 3.7\%$ to $32.1\pm 5.6\%$ in Wt mice (dietary groups merged for values, contralateral vs. ipsilateral, respectively; $P<0.001$) and from $56.78\pm 5.60\%$ to $38.64\pm 5.06\%$ in Tg(apoB-100) mice (dietary groups merged for values, contralateral vs. ipsilateral, respectively; $P<0.004$) due to 1VO (Fig. 10A and B). The microvascular integrity was not altered by either the transgenic genotype or the experimental diet.

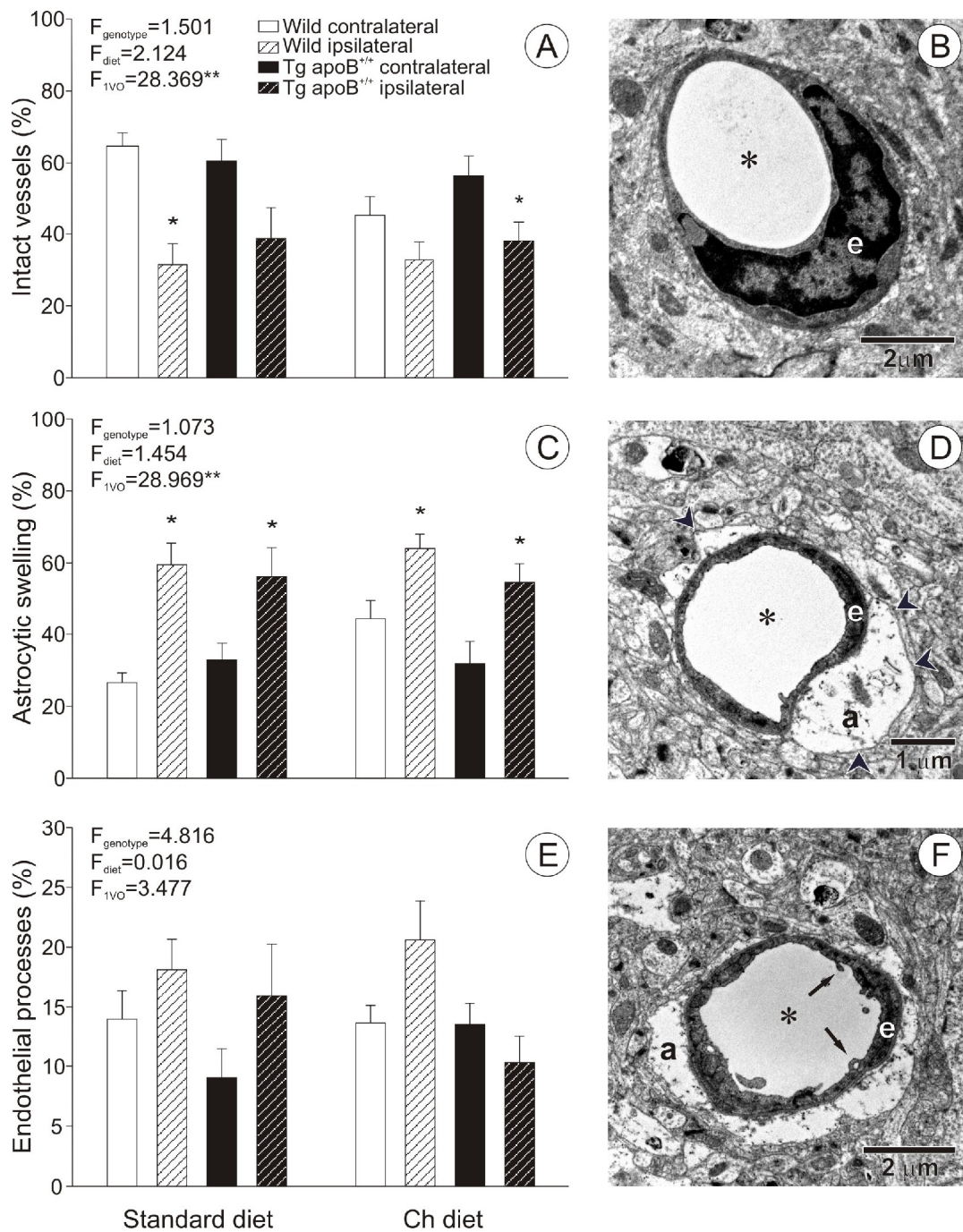


Figure 10. Ultrastructural analysis of cortical capillaries. Representative electron microscopic images of an intact capillary (B), a capillary with swollen astrocytic endfeet (D) and endothelial microvilli (F); the graphs demonstrate the ratio of intact microvessels (A), the ratio of capillaries with pericapillary astrocytic swelling (C), and with endothelial processes (E). Data are given as mean \pm SEM. Statistical analysis was performed with an ANOVA model for three variables (genotype, diet and surgery). The F values for ANOVA are given in the upper left corner in each bar chart, significance levels are defined as $P<0.05^*$ and $P<0.01^{**}$. Abbreviations: 1VO: unilateral common carotid occlusion, a: astrocytic endfeet, asterisk: capillary lumen, arrows (in F): endothelial process, arrowheads (in D): borders of astrocytic swelling, e: endothelial cell, en: endothelial cell nucleus, Tg(apoB-100): human apolipoprotein B-100 expressing transgenic mice, Wt: wild-type mice

Microvascular density appeared significantly lower in Tg(apoB-100) mice as compared with Wt mice (dietary groups merged for values: 195 ± 7 vs. 223 ± 8 vessels/mm²; $P < 0.008$; Fig. 11A), but was not consistently altered by 1VO (comparison between ipsilateral and contralateral cortices; $P < 0.708$). The lumen diameter of the capillaries demonstrated an inverse pattern to the microvascular density. The lumen of cortical capillaries of Tg(apoB-100) mice was significantly more dilated as compared with Wt mice (dietary groups merged for values: 3.16 ± 0.5 vs. 2.88 ± 0.6 μm and $P < 0.001$; Fig. 11B). A tendency in reduction of lumen diameter was observed in the cortex ipsilateral to 1VO as compared with the contralateral side in both Tg(apoB-100) and Wt mice on standard diet; however it did not reach statistical significance ($P < 0.129$). The cholesterol-enriched diet exerted no detectable effect on capillary diameter ($P < 0.925$).

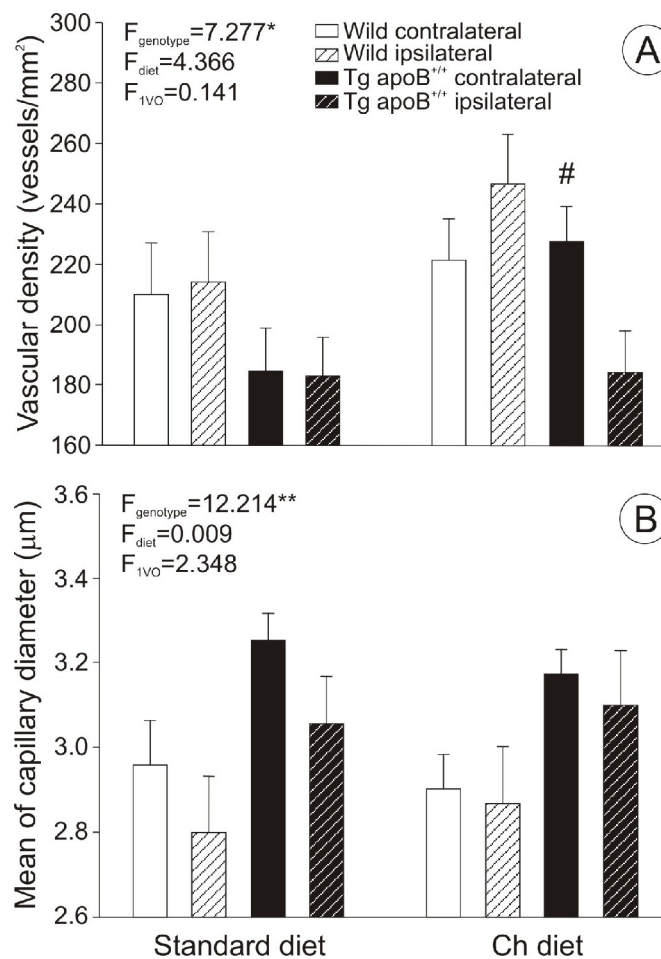


Figure 11. Quantitative data of vascular density (A) and lumen diameter of capillaries (B). Data are given as mean \pm SEM. Significance values for ANOVA are defined as $P < 0.05^*$ and $P < 0.01^{**}$. # (above bars): significant difference ($P < 0.05$) obtained with the Fisher least significant difference (LSD) post hoc test, standard vs. cholesterol-enriched diet. Abbreviations: Tg(apoB-100), human apolipoprotein B-100 expressing transgenic mice; Wt, wild-type mice.

5. DISCUSSION

Injuries of the cerebral microcirculation are hypothesized as either the main or contributing risk factors for the progression of pathophysiologic mechanisms leading to various disease manifestations, such as vascular dementia, AD, neuroinflammation, or hyperlipidemia. The most typical forms of microvascular malformations, which affect the cellular and non-cellular components of the blood-brain barrier (BBB) are basement membrane thickening, perivascular collagen deposition, astrocyte endfoot swelling and the formation of microvillus-like endothelial processes extending into the microvascular lumen. Therefore capillary degeneration in the above pathological states leads to serious functional consequences. First of all, the transport mechanisms through the BBB are hampered and the local regulatory mechanisms are less effective. The partial or complete breakdown of the BBB promotes the non-specific permeability of the BBB, while the facilitated transport of indispensable materials (e.g. glucose, amino acids) is damaged. The opening of the BBB favors different pathologic processes. From the circulatory system, toxic agents are able to traffic into the brain parenchyma, and nutrient supply becomes suboptimal. These processes contribute to cognitive dysfunction, and have been described to be part of the etiology of AD (Abbott et al., 2010; Popescu et al., 2009).

In order to maintain constant and optimal blood supply to the brain through a morphologically compromised cerebrovascular network, compensatory mechanisms must turn on. One possible way to manage normal flow is the adjustment of microvascular density in order for nutrient supply to meet the requirements of the nervous tissue. Vascular remodeling mediated by angiogenesis through vascular endothelial growth factor (VEGF) is considered as a potential mechanism to save brain areas jeopardized by suboptimal nutrient supply through damaged capillary walls. In support of this view, the expression of various angiogenic proteins has been identified in the microvessels of AD brains, as compared with non-demented controls (Thirumangalakudi et al., 2006). In contrast, in the periphery (especially in the myocardium) of hypercholesterolemic rats, Western blot analysis revealed the downregulation of VEGF, which was reversed by resveratrol (Penumathsa 2008). Angiogenesis and vascular remodeling are important elements in several chronic inflammatory diseases; for instance, increased VEGF expression has been found in the spinal cord in a guinea pig model of multiple sclerosis (Kirk and Karlik, 2003).

In addition to the extension of the microvascular network, other mechanism may also compensate for the hindered nutrient supply through a damaged microvascular system.

Increased microvascular caliber may be the maintenance of optimal basal blood flow. Interestingly, arteriolar lumen diameter was found dilated in AD brains (Stopa et al, 2008). Since arterioles are involved in flow regulation rather than nutrient trafficking, the dilated arterioles may promote better blood supply to areas in need in the AD brain.

5.1. Alterations of cerebral white matter microvessels in normal aging and Alzheimer's disease

The main goal of the study was to determine, whether the microvasculature of cerebral periventricular white matter (WM) is injured in AD, and whether the possible microvascular damage appears in the frontal, parietal and occipital white matter areas evenly. The present study on the human post-mortem samples has provided electron microscopic evidence of the microvascular wall pathology in the periventricular WM in AD. Observations of our human study presented the following results. Perivascular fibrous collagen deposition almost linearly increased with advancing age in the FWM and microvascular lumen diameter displayed a linear, positive correlation with age in the PWM. On the other hand, perivascular fibrous collagen accumulation more than tripled in AD patients with neuropathology of Braak V-VI in the PWM.

Numerous experimental observations described WM alterations in cerebral diseases. Between the different subparts of the WM, damage to the periventricular WM is thought to play a role in cognitive failures (Challa et al., 2004), and malformations in the subcortical area are hypothesized to be responsible for depressive symptoms. Various non-invasive imaging techniques helped to identify WM changes in AD and Parkinson's disease (PD). In AD, WM injuries have been described as hypodense areas in computer tomographic (CT) images, while in T2-weighted magnetic resonance imaging (MRI), the same structures appeared as hyperintensive regions (Pantoni and Garcia, 1997). The histopathologic correlates of the WM lesions have been described as myelin rarefaction at light microscopic level. More detailed studies with specific markers confirmed that in the injured WM region, demyelination, apoptotic process of oligodendrocytes and gliosis occur (Brun and Englund, 1986). Such WM malformations are thought to have vascular or ischemic origin. In a number of cases, chronic cerebral hypoperfusion has been shown to play a key role in the evolution of WM rarefaction and dementia (Miki et al, 2009; Farkas et al., 2004). On the other hand, chronic cerebral hypoperfusion is a known process not only in the state of dementia, but also in normal aging.

5.1.1. Cerebral blood flow and microvascular alterations in normal aging

Our data have demonstrated increasing collagen deposition in the microvascular wall with aging, particularly in the FWM. In addition, microvascular lumen diameter was increasingly more dilated with advancing age in the PWM. Chronic cerebral hypoperfusion is proposed to initiate the fine pathology of the microvascular wall, as was shown experimentally in rats with permanent, bilateral common carotid artery occlusion (Farkas and Luiten, 2001). Changes in cerebral perfusion are a well studied phenomenon in various neurodegenerative diseases. Cross-sectional studies on healthy volunteers helped to clarify CBF changes in normal aging (Schultz et al., 1999). When regional, cortical CBF of healthy middle-aged (65-69 years) and old (80-84 years) subjects was compared with the help of SPECT, a significant reduction of about 5% in baseline flow was shown in the parietal and temporal cortex of the old group as compared with the middle-aged group (Claus et al., 1998). The aged had significantly lower CBF, than the younger individuals, and correlation analysis demonstrated that the CBF negatively correlated to life time (Scheel et al., 2000). Most of the data reports the reduction of total CBF in aging and/or dementias, but a CT analysis demonstrated the reduction of the rCBF in WM areas, as well. (Siennicki-Lantz et al., 1998).

Chronically decreased CBF results in lower metabolic rates of oxygen and glucose in the progress of normal aging. Due to insufficient nutrition, all cell types of the brain may undergo degenerative processes. Both the parenchyma, and the fine cerebrovascular network may display structural malformations. The ultrastructure of the microvessels in the aging brain has been investigated with electron microscopy in aging animals; the loss and elongation of the capillary endothelial cells (Mooradian, 1988) and an increased size of pericytic mitochondria was observed, the latter of which was attributed to an active state of the pericytes (Hicks et al, 1983). Besides the cellular elements of the BBB, the basement membrane is also involved in the ultrastructural malformations in aging (Farkas and Luiten, 2001). BM pathologies manifest in the form of BM thickening and fibrous deposition of extracellular matrix components such as collagen, which is suggested to form due to the increased production or the decreased breakdown of the connective tissue elements. In the human periventricular WM, a previous study of ours has identified BM aberrations to correlate markedly with increasing age, especially in the frontal and occipital WM (Farkas et al, 2006). In addition, BM pathology was found to be related to the degree of atherosclerosis that occurred in peripheral vessels such as the aorta (Farkas et al., 2006). Since atherosclerosis

is strongly related to hyperlipidemia, our finding points to investigating the role of hyperlipidemia in cerebral microvascular malformations, which is presented below.

In addition to the fine ultrastructural aberrations, the microvascular architecture may also change with increasing age, but the results in this respect appear to be somewhat controversial. In human neocortex, increased capillary density attributed to tissue shrinkage was observed, but other research groups reported decreased microvascular density in aged humans (Abernethy et al., 1993). We ourselves could not demonstrate any noteworthy association between age and microvascular density in the human periventricular WM (Farkas et al., 2006). However, in animal experiments, a comprehensive comparison of the cortical and hippocampal capillaries of adult and old rats showed that microvascular density was reduced with age (Sonntag et al., 1997). The data available so far on microvascular density in the aging brain, therefore, remain to be inconclusive.

5.1.2. Cerebrovascular pathology in AD

The current analysis of the human samples showed notable perivascular, fibrous collagen deposition in the WM microvascular walls with Braak neuropathology stages V-VI, especially in the PWM region. These results are in agreement with MRI observations in leukoaraiosis (i.e. WM lesions) by Targosz-Gajniak et al. (2009). These authors have demonstrated that WM lesions appeared in all AD patients examined, the amount and size of the WM lesions correlated with age, and that the severity of the lesions in the periventricular WM increased with the progression of AD.

The structural changes of microvessels show here share similar characteristics with those found in capillaries in the cerebral cortex and, more interestingly, in the WM after chronic, experimental, cerebral hypoperfusion in rats (De Jong, 1999; Farkas and Luiten, 2001). In the experimental model of chronic cerebral hypoperfusion, the typical capillary abnormalities included 25% higher occurrence of degenerative pericytes around the blood vessels and 25% higher incidence of basement membrane thickening, with or without fibrosis, in hypoperfused animals. These data demonstrate that decreased cerebral blood flow induces ultrastructural damage of cerebral microvessels (Farkas and Luiten, 2001).

Experimental cerebral hypoperfusion that evokes ischemia has been found to have a deleterious impact on the medullary tissue. The injury appears in the form of glial activation and rarefaction of the WM, as already mentioned under point 5.1. (Farkas et al., 2004; Ueno et al., 2002).

We have additionally shown that the average size of microvascular lumen increases with the severity of AD, especially in the PWM. The increased lumen diameter is suggested to be a compensatory mechanism to maintain normal cerebral perfusion and transport in spite of the increased rigidity and thickness of the microvascular wall as demonstrated by massive collagen deposition.

Our data have demonstrated that the enhanced perivascular accumulation of collagen and the dilation of microvascular lumen in the periventricular WM are region-specific. The most affected site was the parietal region, where the collagen deposition increased most intensely, and the microvascular lumen dilated most noticeably. The microvascular alterations presented here suggest a potentially increased vulnerability of the frontal and parietal areas. Indeed, in normal aging, the reduction of WM integrity as assessed with diffusion tensor imaging was most pronounced in the FWM (Head et al., 2004).

The susceptibility of the frontal and parietal WM to injury may be rooted in the angioarchitecture and perfusion of the region. Accumulating evidence demonstrates that the vascular pattern of WM areas defines perfusion and is related to the metabolic vulnerability of the region (de Reuck, 1971; Farkas et al., 2004; Moody et al., 1990).

5.2. BBB ultrastructure in inflammatory processes

Tumor necrosis factor-alpha (TNF α) is a proinflammatory cytokine, which is produced by various cell types, e.g. macrophages and lymphocytes. TNF α has been demonstrated to cause expression of proadhesive molecules on the endothelium, which results in leukocyte accumulation, adherence, and migration from capillaries into the brain. TNF α promotes inflammation by stimulation of capillary endothelial cell proinflammatory responses and thereby provides leukocyte adhesion and infiltration into the ischemic brain.

TNF α is a well-known and potent vasodilator in various experimental *in vivo* models. The suggested pathway for the vasodilatory influence of TNF α involves nitric-oxide. NOS inhibitors successfully block the vasoactive property of the TNF α (Brian and Faraci, 1998; Shibata et al., 1996).

In addition to the functional role of TNF α in cerebral blood flow regulation, TNF α can impose structural damage to the cerebral microvasculature. In our present study, the ultrastructural analysis of the cerebrocortical capillaries was performed after TNF α treatment in rats. The most obvious aberration concerned the pericapillary astrocytic endfeet, which appeared considerably swollen, seen around the microvessels as distorted, dilated areas

with low electron density in electron microscopic images. Astrocytic swelling is a marked feature not only of inflammatory reactions, but also of seizure-related states (Fabene et al., 2006).

In line with our findings, intracarotid administration of TNF α in newborn piglets resulted in the opening of the BBB. The opening of the BBB in pathologic states can be clearly demonstrated macroscopically after intravenous Evans blue administration (Jancso et al., 1998), or at light microscopic level by sodium fluorescein (Abraham et al., 1996). Evans blue is a vital dye with very high affinity for serum albumin or large molecular weight peptides. Because serum albumin normally cannot cross the BBB, and Evans blue is bound to albumin, albumin-bound Evans blue enters the brain tissue when the BBB has been compromised. Sodium fluorescein labeling is based on the same principle for small molecular weight substances. Besides the different macromolecules labeled by histologic tracers, whole cellular components of the circulating blood are also able to leave the circulation via the impaired BBB. For example, lymphocytes have been shown to transmigrate into the brain parenchyma from the blood after the opening of the BBB by TNF α (Farkas et al., 2003).

An electron microscopic 3-D reconstruction analysis demonstrated that, in normal conditions, the astrocytes cover almost the whole surface of the cerebral vasculature, only small hypothesized microglial processes extend across the perivascular glial sheet to make direct connection with the endothelial cells (Mathiisen et al., 2010). The healthy glial sheet, which is formed by the astrocytes is not just a structural component of the BBB, but also the site of important physiologic processes. The main functions of the mature astrocytes are the maintenance of the extracellular milieu in the brain parenchyma, and the regulation of neurotransmitter level. Normally, the astrocytes are responsible for the re-uptake of glutamate from the synaptic cleft by their specific plasma membrane proteins, which is an activity-dependent mechanism. The excitatory amino acid transporter (EAAT) protein family contribute to this process. The damage of astrocytes influences the level of excitatory neurotransmitters via the alteration of the amount of EAAT sites. Comparative immunohistochemical analysis proved that with the increasing Braak stage a decreased expression of EAAT2 and increased expression of GFAP (i.e. gliosis) occurred (Simpson et al., 2010).

The astrocytes have a main role in the induction of normal formation of brain capillaries. Astrocytes are necessary in endothelial cell cultures to induce BBB phenotype, and experimental evidence have shown that astrocytes induce several BBB properties also in

peripheral endothelial cells (Kuchler-Bopp et al., 1999). Using *in vitro* cell cultures, several specific transport systems are up-regulated in BBB models exposed to astrocytes; however the chemical nature of the inductive signal(s) produced by the astrocytes is currently unclear. The most highly suspected candidates are the glial cell-line derived neurotrophic factors, transforming growth factors- β 1, interleukin-6, and basic fibroblast growth factor (Correale and Villa, 2009), which are involved in the formation of normal BBB phenotype. In addition to the experimental findings described above, the astrocytes play an important role in the clearance and degradation of beta-amyloid plaques in AD (Wyss-Coray et al., 2003), so functionally intact astrocytes may postpone the development of dementia.

Taken together, if the astrocytic endfeet are swollen as shown here, the cross-talk with the endothelium becomes disturbed or discontinues, which can lead to BBB dysfunction. In support of this view, the BBB disruption indicated by the extravasation of Evans blue was associated with astrocytic swelling that involved aquaporin-4, a major water channel implicated in the formation of injury-related brain edema (Venero et al., 2001; Vizuetete et al., 1999).

5.3. The ultrastructure of the BBB in hyperlipidemia and/or ischemia

The first aim of the study was to investigate whether hyperlipidemia (i.e. the expression of human apoB-100 in transgenic mice, and/or cholesterol-rich diet) causes cerebral microvascular lesions. Comparison of the cerebral capillary network proved that the Tg(apoB-100) mice exhibited decreased density and increased capillary lumen diameter as compared with Wt mice. The density of the cerebral capillary network is established during early development, and dynamically reacts to environmental challenges and pathophysiological conditions (e.g. chronic hypoxia leads to increased cerebral capillary density; stroke induces angiogenesis) (Dore-Duffy and LaManna, 2007). The expression of vascular endothelial growth factor is hypothesized as an important determinant of angiogenesis during the development in the brain (Plate, 1999). Genetic hyperlipidemia in rabbits or hypercholesterolemia in mice impaired both basal and stimulated angiogenesis in the ischemic rabbit hindlimb, and in an artificial disk implanted into the thorax of mice (Jang et al., 2000; Van Belle et al., 1997). In these studies the hyperlipidemia-related hindrance of angiogenesis is thought to be an important risk factor for the changed vascular architecture mediated by the VEGF signaling pathway. Alteration of the VEGF–nitric oxide signaling amend the impaired angiogenesis in hypercholesterolemic mice, and the injection of VEGF

re-established angiogenesis in the hyperlipidemic, ischemic rabbit hindlimb (Jang et al., 2000; Van Belle et al., 1997). Therefore, in hyperlipidemic Tg(apoB-100) mice (Chiesa et al., 1993; Csont et al., 2007; Linton et al., 1993; Purcell-Huynh et al., 1995), the capillary density in the cerebral cortex is proposed to be lower due to their high plasma cholesterol or triglyceride profile, thus inhibiting angiogenesis possibly through hampered VEGF signaling.

Parallel with the alteration of the capillary density, the dilation of the capillary lumen was observed. The increase of the lumen diameter is proposed as a complementary and compensatory mechanism in order to maintain standard cerebral perfusion rate (i.e. the normal value of the cerebral blood flow) despite a less dense capillary network in Tg(apoB-100) as compared with Wt mice. With the rearrangement of the microvascular architecture in Tg(apoB-100) mice, altered cerebrovascular reactivity may occur in different pathophysiological conditions, such as ischemia. In addition, a recent study has indicated, that the reduced capillary density may contribute to apoptosis and progressive neuronal cell death in Tg(apoB-100) mice by chronically depriving the brain of its vital nutrients (Bereczki et al., 2008).

The second aim was to determine whether the expression of human apoB-100 in transgenic mice and/or a high-cholesterol diet augment ischemia-related cerebral capillary damage. Unilateral forebrain ischemia was induced by 1VO in Tg(apoB-100) and in Wt mice to answer this question. Previously, 1VO carried out in Mongolian gerbils led to perivascular glial swelling, and irregularities on the luminal vascular surface with endothelial projections (Naganuma, 1990). Similar microvascular pathology has been described in senescence-accelerated mice (Lee et al., 2000; Ueno et al., 1998). Therefore our investigation focused on the ultrastructure of perivascular astrocytic endfeet and the endothelial surface. In the present study, the swelling of astrocytic endfeet and the presence of endothelial microvilli became more prominent in the ischemic hemisphere. These data agree with previous observations made in models of cerebral ischemia: (i) electron microscopic analysis of cerebral microvessels revealed compressed capillaries consistently surrounded by swollen astrocytic endfeet; and (ii) the widespread appearance of cerebral endothelial microvilli (Dietrich et al., 1986). These morphological features imply some harmful functional changes: astrocytic pathology compromises the integrity of the blood–brain barrier (Haseloff et al., 2005), while endothelial microvilli might increase microvascular resistance, leading to moderate hemodynamic impediments (Dietrich et al., 1986).

The data presented here showed that hyperlipidemia in human apoB-100 transgenic mice and chronically elevated dietary cholesterol—alone or in combination—did not have any impact

on capillary ultrastructure in the non-ischemic hemisphere, and did not exacerbate ischemia-induced microvascular lesions in the mouse brain. Morphological description for hyperlipidemia-related vascular pathology has been experimentally demonstrated on larger caliber vessels. For instance, Tg(apoB-100) mice kept on high-fat diet, or hypercholesterolemic rabbits displayed marked atherosclerosis in the aorta (Purcell-Huynh et al., 1995; Sasaki et al., 1988). A comparison between the aorta and cerebral microvessels of hypercholesterolemic rabbits showed that the aorta became atherosclerotic, while the brain microvessels remained free of lipid depositions (Sasaki et al., 1988). Based on these and our data, high serum lipid level-related, morphological, vascular lesions in experimental models are assumed to be confined to large-caliber arteries (e.g. aorta, carotid arteries), rather than cerebral capillaries.

Still, hyperlipidemia may induce biochemical reactions in brain microvessels (Mooradian et al., 1995; Robert et al., 1982). The cerebral capillaries of cholesterol-fed rabbits displayed some biochemical modifications in the capillary walls such as decreased collagen and hexose content (Robert et al., 1982). Also, increased dietary cholesterol enhanced malondialdehyde production in brain microvascular walls in rabbits (Mooradian et al., 1995). Even though high dietary cholesterol thus induces biochemical modifications in the cerebral microvascular endothelial cells, the impact of hyperlipidemia on capillary ultrastructure may not become clearly evident. There has been an ongoing debate whether hyperlipidemia is a direct risk factor for ischemic stroke (Demchuk et al., 1999; Landau, 1999). The data presented here indicate that apoB-100 expression-related hyperlipidemia (both hypercholesterolemia and hypertriglyceridemia) lowers the density of cerebral capillaries, but imposes no obvious ultrastructural microvascular malformations. Cerebral capillary density reduced by high plasma lipid levels as presented here may affect cerebrovascular reactivity during pathophysiological challenges—ischemia being one of the most prominent types.

6. CONCLUSIONS

The studies presented here all aimed to investigate the fine ultrastructure of cerebral capillaries in various pathological conditions that appear as risk factors for AD. First, the morphology of the microvessels of the human cerebral WM in AD was assessed. Second, cerebral microvascular damage as a result of inflammatory processes was characterized. Third, the condition of brain capillaries in severe ischemia and hyperlipidemia was investigated. We have found that, with the exception of hyperlipidemia, the ultrastructure of the BBB becomes compromised in all these conditions, which is suggested to have functional implications. Since the BBB is the site of selective nutrient and waste product trafficking between blood and the nervous tissue, its structural integrity is crucial to fulfill its function and meet the metabolic demands of the central nervous system.

AD is a progressive mental disorder with undefined origin. It has been firmly established that cerebrovascular pathology and chronically reduced cerebral blood flow are hallmarks of AD, cerebral hypoperfusion is a predictive marker of the disease, and that cerebrovascular risk factors contribute to the disintegration of cognitive function over the course of the disease. Our present study confirms the occurrence of microvascular injury in AD brains, and reveals conditions (i.e. ischemia, inflammatory processes), which are causative for the development of cerebral microvascular damage. Our results shed light on the complexity of causative elements that may add up to damage the BBB, and ultimately lead to memory dysfunction.

7. ACKNOWLEDGEMENTS

First of all, I am indebted to my excellent supervisor, **Eszter Farkas, Ph.D.** (Senior Research Associate, Department of Medical Physics and Informatics, Faculty of Medicine, University of Szeged) for her admirable patience and assistance from the initial steps to the final touches of my Ph.D. work throughout.

I would like to express special thanks to **Prof. András Mihály, M.D., Ph.D., D.Sc.** (Professor and Chairman of the Department of Anatomy, Histology and Embryology, Faculty of Medicine, University of Szeged), for his continuous support during my experimental work.

I was honored to be a member of the Cerebrovascular Research Group of **Prof. Ferenc Bari, Ph.D., D.Sc.** (Professor and Chairman of the Department of Medical Physics and Informatics, Faculty of Medicine, University of Szeged). Working in his team has extended my knowledge in the field of cerebrovascular research.

I am grateful to **Zsolt Rázga, Ph.D.** (Research Associate, Department of Pathology, Faculty of Medicine, University of Szeged) and his previous and current assistants, to **Mária Bakacsi** and **Erika Németh** for providing the facilities for EM work, and for the accurate technical help with the use of the EM apparatus.

I am greatly appreciate the support of **Géza G. Kovács, M.D., Ph.D.** (Associate Professor, Institute of Neurology, Medical University of Vienna, Vienna, Austria) and thank him for collecting and offering the post-mortem human samples for our study.

I am thankful to the following assistants of our Department: **Adrienne Mátyás** and **Gabriella Pap** for their caring technical help.

Finally, I would like to give my special thanks to my sister **Erika** and her family for their everyday care and support, and to the prominent members of my circle of friends, namely **Levente Csaba, István Dobó, Antal Radvánszky, Dániel Tari,** and **László Tímár.**

8. REFERENCES

1. Abbott NJ.: Dynamics of CNS barriers: evolution, differentiation, and modulation. *Cell Mol Neurobiol.* 2005; 25(1):5-23.
2. Abbott NJ, Patabendige AA, Dolman DE, Yusof SR, Begley DJ.: Structure and function of the blood-brain barrier. *Neurobiol Dis.* 2010; 37(1):13-25.
3. Abernethy WB, Bell MA, Morris M, Moody DM.: Microvascular density of the human paraventricular nucleus decreases with aging but not hypertension. *Exp Neurol.* 1993; 121(2):270-4.
4. Abraham CS, Deli MA, Joo F, Megyeri P, Torpier G.: Intracarotid tumor necrosis factor-alpha administration increases the blood-brain barrier permeability in cerebral cortex of the newborn pig: quantitative aspects of double-labelling studies and confocal laser scanning analysis. *Neurosci Lett.* 1996;208(2):85-8.
5. Antonelli-Orlidge A, Smith SR, D'Amore PA.: Influence of pericytes on capillary endothelial cell growth. *Am Rev Respir Dis.* 1989; 140(4):1129-31.
6. Arthur FE, Shivers RR, Bowman PD.: Astrocyte-mediated induction of tight junctions in brain capillary endothelium: an efficient in vitro model. *Brain Res.* 1987; 433(1):155-9.
7. Beck DW, Vinters HV, Hart MN, Cancilla PA.: Glial cells influence polarity of the blood-brain barrier. *J Neuropathol Exp Neurol.* 1984 ;43(3):219-24.
8. Bereczki E, Bernát G, Csont T, Ferdinandy P, Scheich H, Sántha M.: Overexpression of human apolipoprotein B-100 induces severe neurodegeneration in transgenic mice. *J Proteome Res.* 2008;7(6):2246-52.
9. Betz AL, Goldstein GW.: Polarity of the blood-brain barrier: neutral amino acid transport into isolated brain capillaries. *Science.* 1978; 202(4364):225-7.
10. Bjelik A, Pákási M, Bereczki E, Gonda S, Juhász A, Rimanóczy A, Zana M, Janka Z, Sántha M, Kálmán J.: APP mRNA splicing is upregulated in the brain of biglycan transgenic mice. *Neurochem Int.* 2007; 50(1):1-4.
11. Blasiola DA, Davis RA, Attie AD.: The physiological and molecular regulation of lipoprotein assembly and secretion. *Mol Biosyst.* 2007; 3(9):608-19.
12. Borroni B, Grassi M, Costanzi C, Archetti S, Caimi L, Padovani A.: APOE genotype and cholesterol levels in lewy body dementia and Alzheimer disease: investigating genotype-phenotype effect on disease risk. *Am J Geriatr Psychiatry.* 2006; 14(12):1022-31.
13. Brian JE Jr, Faraci FM.: Tumor necrosis factor-alpha-induced dilatation of cerebral arterioles. *Stroke.* 1998; 29(2):509-15.

14. Brownlees J, Williams CH.: Peptidases, peptides, and the mammalian blood-brain barrier. *J Neurochem.* 1993; 60(3):793-803.
15. Brownson EA, Abbruscato TJ, Gillespie TJ, Hruby VJ, Davis TP.: Effect of peptidases at the blood brain barrier on the permeability of enkephalin. *J Pharmacol Exp Ther.* 1994; 270(2):675-80.
16. Brun A, Englund E.: A white matter disorder in dementia of the Alzheimer type: a pathoanatomical study. *Ann Neurol.* 1986;19(3):253-62.
17. Cancilla PA, DeBault LE.: Neutral amino acid transport properties of cerebral endothelial cells in vitro. *J Neuropathol Exp Neurol.* 1983; 42(2):191-99.
18. Challa VR, Thore CR, Moody DM, Anstrom JA, Brown WR.: Increase of white matter string vessels in Alzheimer's disease. *J Alzheimers Dis.* 2004; 6(4):379-8.
19. Chiesa G, Johnson DF, Yao Z, Innerarity TL, Mahley RW, Young SG, Hammer RH, Hobbs HH.: Expression of human apolipoprotein B100 in transgenic mice. Editing of human apolipoprotein B100 mRNA. *J Biol Chem.* 1993; 268(32):23747-50.
20. Claus JJ, Breteler MM, Hasan D, Krenning EP, Bots ML, Grobbee DE, Van Swieten JC, Van Harskamp F, Hofman A.: Regional cerebral blood flow and cerebrovascular risk factors in the elderly population. *Neurobiol Aging.* 1998;19(1):57-64.
21. Cohen Z, Molinatti G, Hamel E.: Astroglial and vascular interactions of noradrenaline terminals in the rat cerebral cortex. *J Cereb Blood Flow Metab.* 1997; 17(8):894-904.
22. Coomber BL, Stewart PA.: Morphometric analysis of CNS microvascular endothelium. *Microvasc Res.* 1985; 30(1):99-115.
23. Correale J, Villa A.: Cellular elements of the blood-brain barrier. *Neurochem Res.* 2009; 34(12):2067-77.
24. Csont T, Bereczki E, Bencsik P, Fodor G, Görbe A, Zvara A, Csonka C, Puskás LG, Sántha M, Ferdinandy P.: Hypercholesterolemia increases myocardial oxidative and nitrosative stress thereby leading to cardiac dysfunction in apoB-100 transgenic mice. *Cardiovasc Res.* 2007; 76(1):100-9.
25. De Jong GI, Farkas E, Stienstra CM, Plass JR, Keijser JN, de la Torre JC, Luiten PG.: Cerebral hypoperfusion yields capillary damage in the hippocampal CA1 area that correlates with spatial memory impairment. *Neuroscience.* 1999; 91(1):203-10.
26. de la Torre JC.: Vascular basis of Alzheimer's pathogenesis. *Ann N Y Acad Sci.* 2002; 977:196-215.
27. De Reuck J.: The human periventricular arterial blood supply and the anatomy of cerebral infarctions. *Eur Neurol.* 1971;5(6):321-34.

28. Demchuk AM, Hess DC, Brass LM, Yatsu FM.: Is cholesterol a risk factor for stroke?: Yes. *Arch Neurol.* 1999; 56(12):1518-20.
29. Dietrich WD, Ginsberg MD, Busto R, Watson BD, Yoshida S.: Vascular aspects and hemodynamic consequences of central nervous system injury. *Cent Nerv Syst Trauma.* 1986; 3(4):265-80.
30. Dore-Duffy P, LaManna JC.: Physiologic angiodynamics in the brain. *Antioxid Redox Signal.* 2007; 9(9):1363-71.
31. Duvernoy H, Delon S, Vannson JL.: The vascularization of the human cerebellar cortex. *Brain Res Bull.* 1983; 11(4):419-80.
32. Elhusseiny A, Cohen Z, Olivier A, Stanimirović DB, Hamel E.: Functional acetylcholine muscarinic receptor subtypes in human brain microcirculation: identification and cellular localization. *J Cereb Blood Flow Metab.* 1999; 19(7):794-802.
33. Fabene PF, Weiczner R, Marzola P, Nicolato E, Calderan L, Andrioli A, Farkas E, Süle Z, Mihaly A, Sbarbati A.: Structural and functional MRI following 4-aminopyridine-induced seizures: a comparative imaging and anatomical study. *Neurobiol Dis.* 2006; 21(1):80-9.
34. Farkas E, De Jong GI, Apró E, de Vos RA, Steur EN, Luiten PG.: Similar ultrastructural breakdown of cerebrocortical capillaries in Alzheimer's disease, Parkinson's disease, and experimental hypertension. What is the functional link? *Ann N Y Acad Sci.* 2000; 903:72-82.
35. Farkas E, De Jong GI, de Vos RA, Jansen Steur EN, Luiten PG.: Pathological features of cerebral cortical capillaries are doubled in Alzheimer's disease and Parkinson's disease. *Acta Neuropathol.* 2000; 100(4):395-402.
36. Farkas E, de Vos RA, Donka G, Jansen Steur EN, Mihály A, Luiten PG.: Age-related microvascular degeneration in the human cerebral periventricular white matter. *Acta Neuropathol.* 2006; 111(2):150-7.
37. Farkas E, De Vos RA, Jansen Steur EN, Luiten PG.: Are Alzheimer's disease, hypertension, and cerebrocapillary damage related? *Neurobiol Aging.* 2000; 21(2):235-43.
38. Farkas E, Donka G, de Vos RA, Mihály A, Bari F, Luiten PG.: Experimental cerebral hypoperfusion induces white matter injury and microglial activation in the rat brain. *Acta Neuropathol.* 2004; 108(1):57-64.
39. Farkas E, Luiten PG.: Cerebral microvascular pathology in aging and Alzheimer's disease. *Prog Neurobiol.* 2001; 64(6):575-611.

40. Farkas E, Luiten PG, Bari F.: Permanent, bilateral common carotid artery occlusion in the rat: a model for chronic cerebral hypoperfusion-related neurodegenerative diseases. *Brain Res Rev.* 2007; 54(1):162-80.
41. Farkas IG, Czigner A, Farkas E, Dobó E, Soós K, Penke B, Endrész V, Mihály A.: Beta-amyloid peptide-induced blood-brain barrier disruption facilitates T-cell entry into the rat brain. *Acta Histochem.* 2003; 105(2):115-25.
42. Farrell CL, Pardridge WM.: Blood-brain barrier glucose transporter is asymmetrically distributed on brain capillary endothelial luminal and abluminal membranes: an electron microscopic immunogold study. *Proc Natl Acad Sci U S A.* 1991; 88(13):5779-83.
43. Frank RN, Dutta S, Mancini MA.: Pericyte coverage is greater in the retinal than in the cerebral capillaries of the rat. *Invest Ophthalmol Vis Sci.* 1987; 28(7):1086-91.
44. Franklin KBJ, Paxinos G: *The mouse brain in stereotaxic coordinates.* Academic Press, San Diego, 1997.
45. Gjedde A, Diemer NH.: Double-tracer study of the fine regional blood-brain glucose transfer in the rat by computer-assisted autoradiography. *J Cereb Blood Flow Metab.* 1985; 5(2):282-9.
46. Grundy SM, Vega GL, Kesäniemi YA.: Abnormalities in metabolism of low density lipoproteins associated with coronary heart disease. *Acta Med Scand Suppl.* 1985; 701:23-37.
47. Haseloff RF, Blasig IE, Bauer HC, Bauer H.: In search of the astrocytic factor(s) modulating blood-brain barrier functions in brain capillary endothelial cells in vitro. *Cell Mol Neurobiol.* 2005; 25(1):25-39.
48. Hawkins BT, Davis TP.: *The blood-brain barrier/neurovascular unit in health and disease.* *Pharmacol Rev.* 2005; 57(2):173-85.
49. Head D, Buckner RL, Shimony JS, Williams LE, Akbudak E, Conturo TE, McAvoy M, Morris JC, Snyder AZ.: Differential vulnerability of anterior white matter in nondemented aging with minimal acceleration in dementia of the Alzheimer type: evidence from diffusion tensor imaging. *Cereb Cortex.* 2004; 14(4):410-23.
50. Hellström M, Gerhardt H, Kalén M, Li X, Eriksson U, Wolburg H, Betsholtz C.: Lack of pericytes leads to endothelial hyperplasia and abnormal vascular morphogenesis. *J Cell Biol.* 2001; 153(3):543-53.
51. Hicks P, Rolsten C, Brizzee D, Samorajski T.: Age-related changes in rat brain capillaries. *Neurobiol Aging.* 1983;4(1):69-75.

52. Hirao K, Ohnishi T, Hirata Y, Yamashita F, Mori T, Moriguchi Y, Matsuda H, Nemoto K, Imabayashi E, Yamada M, Iwamoto T, Arima K, Asada T.: The prediction of rapid conversion to Alzheimer's disease in mild cognitive impairment using regional cerebral blood flow SPECT. *Neuroimage*. 2005; 28(4):1014-21.
53. Jancsó G, Domoki F, Sántha P, Varga J, Fischer J, Orosz K, Penke B, Becskei A, Dux M, Tóth L.: Beta-amyloid (1-42) peptide impairs blood-brain barrier function after intracarotid infusion in rats. *Neurosci Lett*. 1998; 253(2):139-41.
54. Jang JJ, Ho HK, Kwan HH, Fajardo LF, Cooke JP.: Angiogenesis is impaired by hypercholesterolemia: role of asymmetric dimethylarginine. *Circulation*. 2000; 102(12):1414-9.
55. Kirk SL, Karlik SJ.: VEGF and vascular changes in chronic neuroinflammation. *J Autoimmun*. 2003;21(4):353-63.
56. Krämer SD, Abbott NJ, Begley DJ: Biological models to study blood–brain barrier permeation. In: *Pharmacokinetic Optimization in Drug Research: Biological, Physicochemical and Computational Strategies*. 2001; 127-153
57. Kuchler-Bopp S, Delaunoy JP, Artault JC, Zaepfel M, Dietrich JB.: Astrocytes induce several blood-brain barrier properties in non-neural endothelial cells. *Neuroreport*. 1999; 10(6):1347-53.
58. Landau WM.: Is cholesterol a risk factor for stroke?: No. *Arch Neurol*. 1999; 56(12):1521-4.
59. Lee EY, Lee SY, Lee TS, Chi JG, Choi W, Suh YH.: Ultrastructural changes in microvessel with age in the hippocampus of senescence-accelerated mouse (SAM)-P/10. *Exp Aging Res*. 2000; 26(1):3-14.
60. Libby P.: Fat fuels the flame: triglyceride-rich lipoproteins and arterial inflammation. *Circ Res*. 2007; 100(3):299-301.
61. Linton MF, Farese RV Jr, Chiesa G, Grass DS, Chin P, Hammer RE, Hobbs HH, Young SG.: Transgenic mice expressing high plasma concentrations of human apolipoprotein B100 and lipoprotein(a). *J Clin Invest*. 1993; 92(6):3029-37.
62. Luiten PG, de Jong GI, Van der Zee EA, van Dijken H.: Ultrastructural localization of cholinergic muscarinic receptors in rat brain cortical capillaries. *Brain Res*. 1996; 720(1-2):225-9.
63. Magaki S, Mueller C, Dickson C, Kirsch W.: Increased production of inflammatory cytokines in mild cognitive impairment. *Exp Gerontol*. 2007; 42(3):233-40.

64. Mathiisen TM, Lehre KP, Danbolt NC, Ottersen OP.: The perivascular astroglial sheath provides a complete covering of the brain microvessels: an electron microscopic 3D reconstruction. *Glia*. 2010; 58(9):1094-1103.
65. Matsuda H.: Cerebral blood flow and metabolic abnormalities in Alzheimer's disease. *Ann Nucl Med*. 2001; 15(2):85-92.
66. McNaull BB, Todd S, McGuinness B, Passmore AP.: Inflammation and anti-inflammatory strategies for Alzheimer's disease--a mini-review. *Gerontology*. 2010; 56(1):3-14.
67. Miki K, Ishibashi S, Sun L, Xu H, Ohashi W, Kuroiwa T, Mizusawa H.: Intensity of chronic cerebral hypoperfusion determines white/gray matter injury and cognitive/motor dysfunction in mice. *J Neurosci Res*. 2009;87(5):1270-81.
68. Minn A, Ghersi-Egea JF, Perrin R, Leininger B, Siest G.: Drug metabolizing enzymes in the brain and cerebral microvessels. *Brain Res Brain Res Rev*. 1991; 16(1):65-82.
69. Moody DM, Bell MA, Challa VR.: Features of the cerebral vascular pattern that predict vulnerability to perfusion or oxygenation deficiency: an anatomic study. *AJNR Am J Neuroradiol*. 1990;11(3):431-9.
70. Mooradian AD.: Effect of aging on the blood-brain barrier. *Neurobiol Aging*. 1988; 9(1):31-9.
71. Mooradian AD, Lung CC, Pinnas JL.: Cholesterol enriched diet enhances malondialdehyde modification of proteins in cerebral microvessels of rabbits. *Neurosci Lett*. 1995; 185(3):211-3.
72. Naganuma Y.: Changes of the cerebral microvascular structure and endothelium during the course of permanent ischemia. *Keio J Med*. 1990; 39(1):26-31.
73. Oldendorf WH, Cornford ME, Brown WJ.: The large apparent work capability of the blood-brain barrier: a study of the mitochondrial content of capillary endothelial cells in brain and other tissues of the rat. *Ann Neurol*. 1977; 1(5):409-17.
74. Olofsson SO, Boren J.: Apolipoprotein B: a clinically important apolipoprotein which assembles atherogenic lipoproteins and promotes the development of atherosclerosis. *J Intern Med*. 2005; 258(5):395-410.
75. Oomen CA, Farkas E, Roman V, van der Beek EM, Luiten PG, Meerlo P.: Resveratrol preserves cerebrovascular density and cognitive function in aging mice. *Front Aging Neurosci*. 2009; 1:4.
76. Pantoni L, Garcia JH.: Cognitive impairment and cellular/vascular changes in the cerebral white matter. *Ann N Y Acad Sci*. 1997; 826:92-102.

77. Paxinos G, Watson C: *The Rat Brain in Stereotactic Coordinates*, 2nd ed., Academic Press, New York, 1986.
78. Penumathsa SV, Koneru S, Samuel SM, Maulik G, Bagchi D, Yet SF, Menon VP, Maulik N.: Strategic targets to induce neovascularization by resveratrol in hypercholesterolemic rat myocardium: role of caveolin-1, endothelial nitric oxide synthase, hemeoxygenase-1, and vascular endothelial growth factor. *Free Radic Biol Med.* 2008;45(7):1027-34.
79. Peppiatt CM, Howarth C, Mobbs P, Attwell D.: Bidirectional control of CNS capillary diameter by pericytes. *Nature.* 2006; 443(7112):700-4.
80. Persson J, Nilsson J, Lindholm MW.: Cytokine response to lipoprotein lipid loading in human monocyte-derived macrophages. *Lipids Health Dis.* 2006; 5:17.
81. Plaschke K, Staub J, Ernst E, Marti HH.: VEGF overexpression improves mice cognitive abilities after unilateral common carotid artery occlusion. *Exp Neurol.* 2008; 214(2):285-92.
82. Plate KH.: Mechanisms of angiogenesis in the brain. *J Neuropathol Exp Neurol.* 1999; 58(4):313-20.
83. Popescu BO, Toescu EC, Popescu LM, Bajenaru O, Muresanu DF, Schultzberg M, Bogdanovic N.: Blood-brain barrier alterations in ageing and dementia. *J Neurol Sci.* 2009; 283(1-2):99-106
84. Purcell-Huynh DA, Farese RV Jr, Johnson DF, Flynn LM, Pierotti V, Newland DL, Linton MF, Sanan DA, Young SG.: Transgenic mice expressing high levels of human apolipoprotein B develop severe atherosclerotic lesions in response to a high-fat diet. *J Clin Invest.* 1995; 95(5):2246-57.
85. Robert AM, Miskulin M, Godeau G, Tixier JM, Milhaud G.: Action of calcitonin on the atherosclerotic modifications of brain microvessels induced in rabbits by cholesterol feeding. *Exp Mol Pathol.* 1982; 37(1):67-73.
86. Rubin LL, Hall DE, Porter S, Barbu K, Cannon C, Horner HC, Janatpour M, Liaw CW, Manning K, Morales J, Tanner LI, Tomaselli KJ, Bard F.: A cell culture model of the blood-brain barrier. *J Cell Biol.* 1991; 115(6):1725-35.
87. Rudel LL, Parks JS, Johnson FL, Babiak J.: Low density lipoproteins in atherosclerosis. *J Lipid Res.* 1986; 27(5):465-74.
88. Sasaki N, Saito Y, Yosida S.: Effect of hypercholesterolemia on cholinephosphotransferase activity in rabbit and rat vessel walls. *Atherosclerosis.* 1988; 74(3):241-6.

89. Scheel P, Ruge C, Petruch UR, Schöning M.: Color duplex measurement of cerebral blood flow volume in healthy adults. *Stroke*. 2000;31(1):147-50.
90. Schultz SK, O'Leary DS, Boles Ponto LL, Watkins GL, Hichwa RD, Andreasen NC.: Age-related changes in regional cerebral blood flow among young to mid-life adults. *Neuroreport*. 1999; 10(12):2493-6.
91. Shibata M, Parfenova H, Zuckerman SL, Leffler CW.: Tumor necrosis factor-alpha induces pial arteriolar dilation in newborn pigs. *Brain Res Bull*. 1996; 39(4):241-7.
92. Siennicki-Lantz A, Lilja B, Rosén I, Elmstahl S.: Cerebral blood flow in white matter is correlated with systolic blood pressure and EEG in senile dementia of the Alzheimer type. *Dement Geriatr Cogn Disord*. 1998; 9(1):29-38.
93. Silvestrini M, Paolino I, Vernieri F, Pedone C, Baruffaldi R, Gobbi B, Cagnetti C, Provinciali L, Bartolini M.: Cerebral hemodynamics and cognitive performance in patients with asymptomatic carotid stenosis. *Neurology*. 2009; 72(12):1062-8.
94. Simpson JE, Ince PG, Lace G, Forster G, Shaw PJ, Matthews F, Savva G, Brayne C, Wharton SB: Astrocyte phenotype in relation to Alzheimer-type pathology in the ageing brain. *Neurobiol Aging*. 2010; 31(4):578-90.
95. Song F, Poljak A, Smythe GA, Sachdev P.: Plasma biomarkers for mild cognitive impairment and Alzheimer's disease. *Brain Res Rev*. 2009; 61(2):69-80.
96. Sonntag WE, Lynch CD, Cooney PT, Hutchins PM.: Decreases in cerebral microvasculature with age are associated with the decline in growth hormone and insulin-like growth factor 1. *Endocrinology*. 1997;138(8):3515-20.
97. Sparks DL.: The early and ongoing experience with the cholesterol-fed rabbit as a model of Alzheimer's disease: the old, the new and the pilot. *J Alzheimers Dis*. 2008; 15(4):641-56.
98. Sparks DL, Kryscio RJ, Sabbagh MN, Connor DJ, Sparks LM, Liebsack C.: Reduced risk of incident AD with elective statin use in a clinical trial cohort. *Curr Alzheimer Res*. 2008; 5(4):416-21.
99. Stopa EG, Butala P, Salloway S, Johanson CE, Gonzalez L, Tavares R, Hovanesian V, Hulette CM, Vitek MP, Cohen RA.: Cerebral cortical arteriolar angiopathy, vascular beta-amyloid, smooth muscle actin, Braak stage, and APOE genotype. *Stroke*. 2008 Mar;39(3):814-21.
100. Süle Z, Mracskó E, Bereczki E, Sántha M, Csont T, Ferdinandy P, Bari F, Farkas E.: Capillary injury in the ischemic brain of hyperlipidemic, apolipoprotein B-100 transgenic mice. *Life Sci*. 2009; 84(25-26):935-9.

101. Targosz-Gajniak M, Siuda J, Ochudło S, Opala G.: Cerebral white matter lesions in patients with dementia - from MCI to severe Alzheimer's disease. *J Neurol Sci.* 2009; 283(1-2):79-82.
102. Thirumangalakudi L, Samany PG, Owoso A, Wiskar B, Grammas P.: Angiogenic proteins are expressed by brain blood vessels in Alzheimer's disease. *J Alzheimers Dis.* 2006;10(1):111-8.
103. Ueno M, Akiguchi I, Hosokawa M, Shinnou M, Sakamoto H, Takemura M, Higuchi K.: Ultrastructural and permeability features of microvessels in the olfactory bulbs of SAM mice. *Acta Neuropathol.* 1998; 96(3):261-70.
104. Ueno M, Tomimoto H, Akiguchi I, Wakita H, Sakamoto H.: Blood-brain barrier disruption in white matter lesions in a rat model of chronic cerebral hypoperfusion. *J Cereb Blood Flow Metab.* 2002; 22(1):97-104.
105. Van Belle E, Rivard A, Chen D, Silver M, Bunting S, Ferrara N, Symes JF, Bauters C, Isner JM.: Hypercholesterolemia attenuates angiogenesis but does not preclude augmentation by angiogenic cytokines. *Circulation.* 1997; 96(8):2667-74.
106. van Exel E, Eikelenboom P, Comijs H, Frölich M, Smit JH, Stek ML, Scheltens P, Eefsting JE, Westendorp RG.: Vascular factors and markers of inflammation in offspring with a parental history of late-onset Alzheimer disease. *Arch Gen Psychiatry.* 2009; 66(11):1263-70.
107. van Oijen M, de Jong FJ, Witteman JC, Hofman A, Koudstaal PJ, Breteler MM.: Atherosclerosis and risk for dementia. *Ann Neurol.* 2007; 61(5):403-10.
108. Venero JL, Vizuete ML, Machado A, Cano J.: Aquaporins in the central nervous system. *Prog Neurobiol.* 2001;63(3):321-36.
109. Vizuete ML, Venero JL, Vargas C, Ilundáin AA, Echevarría M, Machado A, Cano J.: Differential upregulation of aquaporin-4 mRNA expression in reactive astrocytes after brain injury: potential role in brain edema. *Neurobiol Dis.* 1999;6(4):245-58.
110. Wyss-Coray T, Loike JD, Brionne TC, Lu E, Anankov R, Yan F, Silverstein SC, Husemann J.: Adult mouse astrocytes degrade amyloid-beta in vitro and in situ. *Nat Med.* 2003; 9(4):453-7.
111. Yoshizaki K, Adachi K, Kataoka S, Watanabe A, Tabira T, Takahashi K, Wakita H.: Chronic cerebral hypoperfusion induced by right unilateral common carotid artery occlusion causes delayed white matter lesions and cognitive impairment in adult mice. *Exp Neurol.* 2008; 210(2):585-91.

9. APPENDIX

COPIES OF PUBLICATIONS, RELATED TO THIS THESIS

- I. Fabene PF, Weiczner R, Marzola P, Nicolato E, Calderan L, Andrioli A, Farkas E, **Süle Z**, Mihály A, Sbarbati A: Structural and functional MRI following 4-aminopyridine-induced seizures: a comparative imaging and anatomical study.
Neurobiol Dis. 2006 Jan; 21(1):80-9
- II. Farkas E, **Süle Z**, Tóth-Szűki V, Mátyás A, Antal P, Farkas IG, Mihály A, Bari F: Tumor necrosis factor-alpha increases cerebral blood flow and ultrastructural capillary damage through the release of nitric oxide in the rat brain.
Microvasc Res. 2006 Nov; 72(3):113-9
- III. **Süle Z**, Mracskó É, Bereczki E, Sántha M, Csont T, Ferdinándy P, Bari F, Farkas E: Capillary injury in the ischemic brain of hyperlipidemic, apolipoprotein B-100 transgenic mice.
Life Sci. 2009 Jun 19; 84(25-26):935-9

COPIES OF ABSTRACTS PUBLISHED IN CITED JOURNALS, RELATED TO THIS THESIS

- i. **Süle Z**, Tóth-Szűki V, Antal P, Mátyás A, Mihály A, Bari F, Farkas E: TNF- α -induced microvascular damage is mediated by nitrogen monoxide in the rat brain.
Clin. Neurosci./Ideggyógy. Szle. 2006, 59 (1 klsz.)
- ii. **Süle Z**, Bari F, Sántha M, Bereczki E, Farkas E: Capillary injury in the ischemic brain of hyperlipidemic, apolipoprotein b-100 transgenic mice.
J. Vasc. Res., 2008, 45, (Suppl. 2), 122
- iii. **Süle Z**, Kovács GG, Mihály A, Farkas E: Microvascular aberrations in the white matter in Alzheimer's disease.
J. Neurol. Sci., 2009, 283, (1-2), 286